THE JOURNAL OF COMPARATIVE NEUROLOGY 399:269–288 (1998)

The Zeta Cell: A New Ganglion Cell Type in Cat Retina

D.M. BERSON,* M. PU, AND E.V. FAMIGLIETTI
Department of Neuroscience, Brown University, Providence, Rhode Island 02912

ABSTRACT

We define a new morphological type of ganglion cell in cat retina by using intracellular staining in vitro. The zeta cell has a small soma, slender axon, and compact, tufted, unistratified dendritic arbor. Dendritic fields were intermediate in size among cat ganglion cells, typically twice the diameter of beta cell fields. They were smallest in the nasal visual streak (<280 μm diameter), especially near the area centralis (60–150 μm diameter), and largest in the nonstreak periphery (maximum diameter 570 μm). Fields sizes were symmetric about the nasotemporal raphe except near the visual streak, where nasal fields were smaller than temporal ones. Zeta-cell dendrites ramified near the boundary between sublaminae *a* and *b* (OFF and ON sublayers) of the inner plexiform layer, occupying the narrow gap separating the dendrites of ON and OFF alpha cells. There was no evidence for separate ON and OFF types of zeta cell. Retrograde labeling studies revealed that both nasally and temporally located zeta cells project to the contralateral superior colliculus, whereas few project to the ipsilateral colliculus or to any subdivision of the dorsal lateral geniculate nucleus. The zeta cell's morphology and projection patterns suggest that it corresponds to the ON-OFF phasic W-cell (also known as the local edge detector) of physiological studies. Zeta cells have particularly small dendritic fields in the visual streak, presumably because they are disproportionately represented in the streak in comparison with other ganglion cell types. These conditions are consistent with optimal spatial resolution along the retinal projection of the visual horizon rather than principally at the center of gaze. Strong commonalities with similar ganglion cell types in ferret, rabbit, and monkey suggest that "zeta-like" cells may be a universal feature of the mammalian retina. J. Comp. Neurol. 399:269–288, 1998.

Indexing terms: gamma cell; W-cell; visual streak; local edge detector; superior colliculus

The outflow of visual information from vertebrate retina arises from a large number of distinct ganglion cell types. Defining these types and characterizing their anatomical and functional specializations represents a crucial step in understanding the parallel organization of the visual pathways. Comprehensive descriptions of single ganglion cell types, correlating morphology, response properties, and afferent and efferent connectivity, are available for only a small minority of the ganglion cell types presumed to exist in any vertebrate retina (e.g., Rodieck, 1979, 1988; Stone, 1983; Dowling, 1987; Amthor et al., 1989; Wässle and Boycott, 1991; Rodieck and Watanabe, 1993). Even at a purely morphological level, progress in ganglion-cell typology has been remarkably slow. Although many ganglion cell forms have been documented, most have yet to be subjected to a formal classification that encompasses somadendritic architecture and stratification, topographic variations in the mosaic formed by homotypic cells, and patterns of central projection. In cat retina, this ideal has been approached for only alpha, beta, epsilon, and delta (monoamine-accumulating) cells, and physiological identities have only been established directly for the first three of these (Boycott and Wässle, 1974; Famiglietti and Kolb, 1976; Leventhal et al., 1980; Kolb et al., 1981; Wässle et al., 1981; Saito, 1983; Fukuda et al., 1984; Leventhal et al., 1985; Dacey, 1989; Wässle and Boycott, 1991; Pu et al., 1994).

In the present report, we use intracellular staining and retrograde labeling to define a new morphological type of ganglion cell in the cat retina. This cell is designated the zeta cell, extending the Greek alphabetical series intro-

Grant sponsor: National Eye Institute; Grant number: PHS 5 R01 EY06108.

Dr. Pu's current address: Department of Neurobiology and Anatomy, University of Utah College of Medicine, Salt Lake City, UT 84132.

*Correspondence to: David M. Berson, Department of Neuroscience, Box 1953, Brown University, Providence, RI 02912.
E-mail: David_Berson@Brown.edu

Received 23 February 1998; Revised 19 May 1998; Accepted 26 May 1998

duced for morphologically defined types of cat ganglion cells by Boycott and Wässle (1974).

MATERIALS AND METHODS

Dye injection and histochemistry

Ganglion cells were stained by intracellular injection of Lucifer Yellow and either biocytin or Neurobiotin in the living retina in vitro using previously described methods (Pu and Berson, 1992; Pu et al., 1994). These methods were approved by Brown University's Institutional Animal Care and Use Committee and conformed with National Institutes of Health guidelines. Cats were deeply anesthetized with Nembutal (35 mg/kg ip) and, following eye removal, killed by Nembutal overdose with or without vascular perfusion with paraformaldehyde. Retinas were isolated and superfused at room temperature with oxygenated Ames medium (Sigma, St. Louis, MO), and intracellular impalements were made under visual control. In some experiments, we injected cells that had been tagged by retrograde transport of fluorescent latex microspheres deposited in the superior colliculus (15 retinas from 9 cats) or various subdivisions of the lateral geniculate nucleus (17 retinas from 10 cats) as described elsewhere (Pu and Berson, 1991, 1992; Pu et al., 1994; Stein et al., 1996). In other experiments (30 retinas from 21 cats), we targeted ganglion cells stained supravitally with acridine orange (see Pu et al., 1994 for details). For the analysis of dendritic stratification, we sometimes impaled and stained one or more marker or "fiducial" cells (Famiglietti, 1992b) in the vicinity of filled zeta cells. Usually alpha cells were chosen for this purpose because they have relatively narrowly stratified dendritic fields (Famiglietti and Kolb, 1976; Kolb et al., 1981; Wässle et al., 1981; Freed and Sterling, 1988; Dacey, 1989; Kolb and Nelson, 1993) and large somata that made it easy to target them for intracellular staining in vitally dyed retinas. In addition, a variety of other ganglion cell types, including beta, delta (monoamine-accumulating), and epsilon cells, were stained in these experiments and were used for comparisons in dendritic field size and stratification.

Retinas were fixed for several hours in 4% buffered paraformaldehyde pH 7.4, processed immunohistochemically (Pu and Berson, 1992), and mounted on glass slides. In early experiments, retinas were dehydrated, cleared, and coverslipped with Permount. This produced negligible linear shrinkage in the plane of the wholemount (Pu et al., 1994), but marked shrinkage in depth. In later experiments, retinas were coverslipped with buffered glycerol, pH 7.4, without prior dehydration or clearing to minimize shrinkage in depth. Quantitative analysis of stratification was carried out exclusively in such hydrated material. Dry objective lenses were used, so optical foreshortening produced at the air/glass interface (Snell's law) has been corrected by multiplying apparent depth values by 1.52 (Williams and Rakic, 1988). Because of the small difference in refractive index between glycerol (1.47) and glass (1.52), depth values may be overestimated by as much as 5%.

Microscopic analysis

Ganglion cells were visible throughout most retinas without counterstaining by virtue of nonspecific histochemical labeling. This, together with vascular patterns in the central retina, allowed us to determine the coordinates of the area centralis and of points on the axis of the visual streak in the nasal periphery. The axis of the visual streak was taken to be a straight line passing through the area centralis and a point on the streak. The axis thus defined had the expected relationship to the optic disk (e.g., Hughes, 1981; Stone, 1983). We estimate that errors in localization were <300 µm for the area centralis, <700 µm for the visual streak, and typically much less for both.

Diameters of dendritic fields and somata were taken as the mean of the maximal and minimal diameters as measured with an eyepiece graticule. Dendritic field measurements were made only in cells judged to be fully stained. For the great majority of cells, a general impression of the depth of dendritic stratification could be obtained by through-focus analysis. One cue was the depth of dendrites relative to the ganglion cell layer, which was visible from background staining of cell bodies. In many cases, the innermost neurons of the inner nuclear layer (INL) could also be resolved by using oblique illumination. An alternative marker for the inner margin of the INL was a characteristic array of dark brown granules. The granules were small (~1 µm diam.), typically round, and occurred at densities ranging from roughly 5,000/mm^2 in the central retina to 1,200/mm^2 in the far periphery. We have not determined the identity of these elements, but their hue suggests that they have been marked by the diaminobenzidine reaction product, perhaps as a result of endogenous oxidative activity or affinity for one of the antibodies. In wholemounts, they lay in the same plane of focus as the innermost somatic profiles (amacrine cells) of the inner INL. They appeared to lie mainly outside the perikarya of these cells, although rarely an intrasomatic site seemed more likely. By using these fiducial marks, it was almost always possible using through-focus analysis to determine with confidence whether a stained alpha or beta cell belonged to the *a* (OFF) or *b* (ON) subtypes. For many of the alpha cells, this judgment could be confirmed because of overlap with another intracellularly stained alpha cell of opposite type.

RESULTS

Zeta cells had relatively small somata, slender axons, and highly branched dendritic fields that were intermediate in size among cat ganglion cells (60–570 µm; Figs. 1, 2). The camera lucida drawings of Figure 1 illustrate the form of representative zeta cells at various retinal locations, and the photomicrographs of Figure 2 display some of the morphological features of these cells.

Somatic and axonal morphology

Zeta cell somata were ovoid or round and substantially smaller than those of most other cat ganglion cells (Figs. 2G,H, 3A), ranging in diameter from 11 to 20 µm (mean: 16.0 µm $\pm$ 1.7 s.d.; n = 154; Fig. 3A). Except for the smaller somata in the extreme central retina, there was no obvious variation in soma size with retinal eccentricity (Fig. 3B) or distance from the visual streak (Fig. 3C; see below).

Axons of zeta cells almost always emerged from the soma. They were invariably very slender, apparently less than 1 µm in diameter, although a more quantitative statement is precluded by optical limitations. They appeared finer than those of cat beta, epsilon, and delta (monoamine-accumulating) types stained by the same methods (Fig. 2I,J). Well-stained zeta cell axons almost

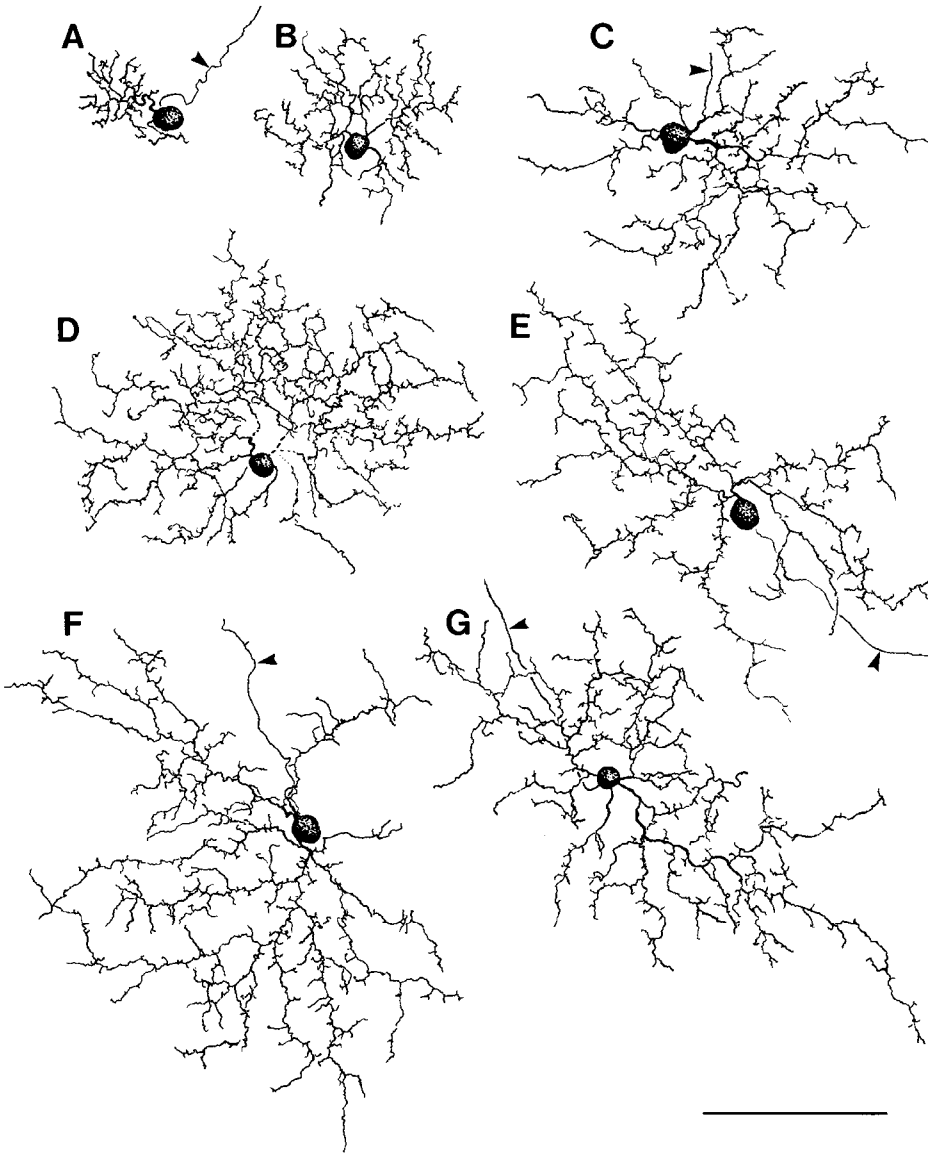

Fig. 1. **A–J:** Camera lucida drawings of stained zeta cells in retinal wholemounts. Arrowheads indicate axons. Photomicrographs of cell in H appear in Figure 2F and I. Eccentricities (e) and distances from the visual streak axis (s) in millimeters as follows: A: e = +0.3, s = +0.3; B: e = -0.4, s = -0.0; C: e = +9.4, s = +0.0; D: e = +1.9, s = +1.9; E: e = +6.4, s = -0.2; F: e = +12.2, s = -1.0; G: e = +9.1, s = -0.6; H: e = +10.9, s = +1.5; I: e = +11.5, s = -3.3; J: e = -5.6, s = +4.8. Negative eccentricities denote locations in temporal hemiretina, negative streak values denote locations in inferior hemiretina. Cells in C,E,G,H, and I were labeled by retrograde transport from the contralateral superior colliculus. All drawings are at the same scale. Scale bar = 100 μm.

always gave rise to at least one and more typically three to five very thin short side branches (Figs. 1H, 2I). These lacked spines or varicosities, were usually only a few micrometers in length, and were restricted to the optic fiber layer. Although most common within a few hundred micrometers of the soma, they could be observed as far as 1 mm away in some cells. We have observed such axonal branches, although far less frequently, among other varieties of non-alpha, non-beta ganglion cells of the cat retina.

Dendritic morphology

Typically one to four primary dendrites of moderately fine caliber emerged from the soma. Dendritic branching was abundant and somewhat irregular. Within much of the dendritic field, branching frequency increased with distance from the cell body, a pattern designated elsewhere as "tufted" (Ramón-Moliner, 1962; Famiglietti, 1992a). Most cells possessed a profusion of irregular dendritic appendages consisting of spines, knobby swellings, spicules, and complex appendages (Fig. 2D–F). Most were short, but others were long enough (>5 μm) that the distinction between them and short dendritic branches was arbitrary. The high density of both branching and appendages gave much of the field a bushy appearance. Toward the irregular perimeter of most dendritic fields, however, it was common to find some sparsely branched processes; these could nonetheless be studded with appendages (Fig. 2). There was a moderate degree of dendritic

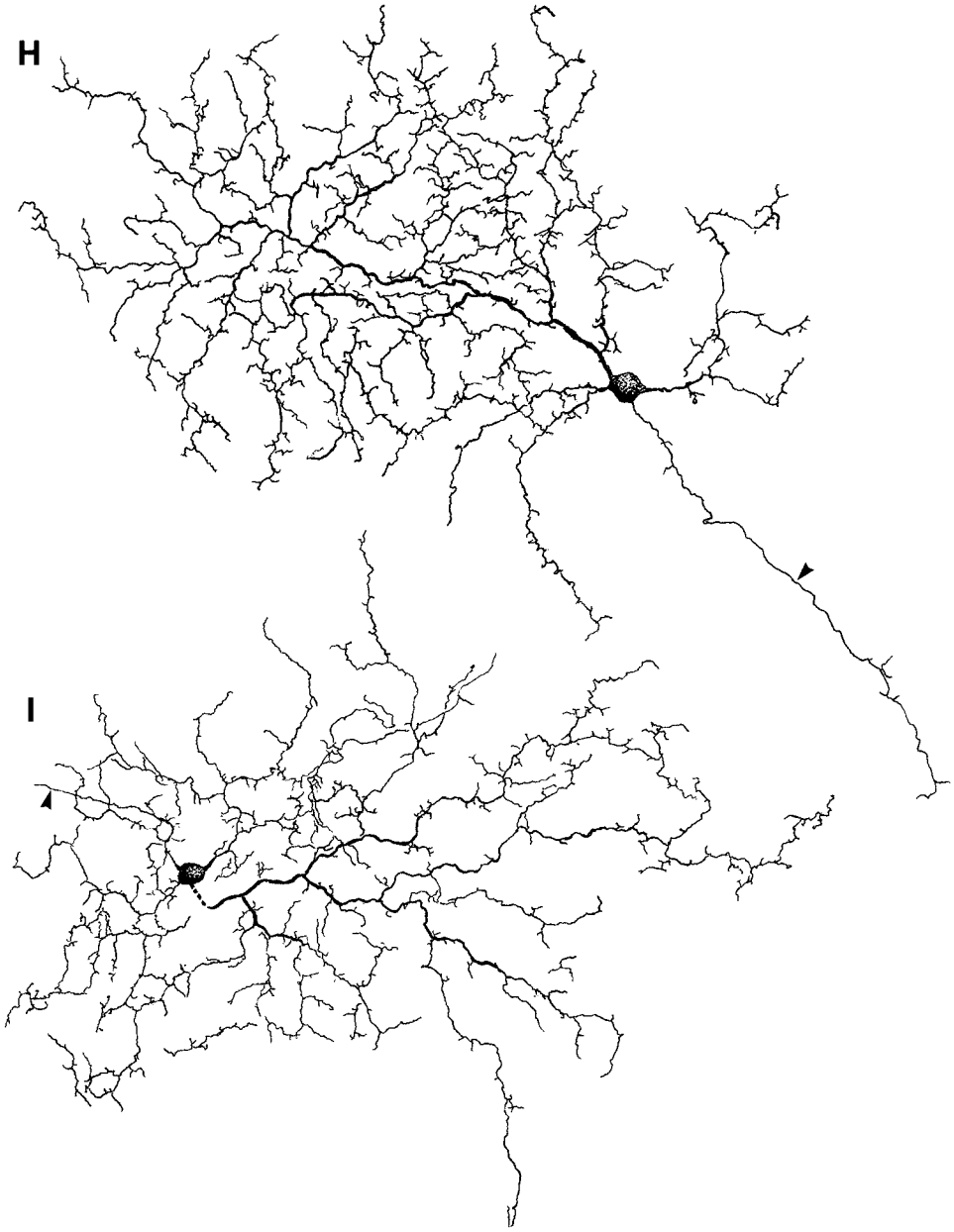

Figure 1 (Continued)

waviness at fairly high spatial frequency, contributing to the bushy impression. However, the overall course of dendritic branches was typically straight, rather than recurving. Thus, frank overlap among dendrites was unusual, although terminal processes commonly ended very near one another and occasionally made apparent contact.

Dendritic perimeters ranged from roughly circular to distinctly elliptical. The soma could be centered within this perimeter (e.g., Fig. 1E,G) or eccentrically located, even radically so (e.g., Fig. 1A,H). These variations seemed largely independent of retinal topography, although elongated dendritic profiles tended to have long axes radially oriented with respect to the area centralis, as for other cat ganglion cell types (Leventhal and Schall, 1983; Pu et al., 1994).

Topographic variations in dendritic field size

Topographic variations in the size of zeta cell dendritic fields were analyzed in terms of retinal eccentricity (radial distance from the center of the area centralis) and distance superior or inferior from the visual streak, a horizontal band of elevated ganglion cell density that passes through the area centralis. Field size was related to eccentricity (Fig. 4A). Only cells with small fields (<220 μm in diameter) were observed in the central retina (<2 mm eccentricity), whereas cells with the largest fields (>400 μm diameter) invariably lay in the retinal periphery (>4 mm eccentricity). In the nasal retina, however, the relationship was surprisingly weak. In the far nasal periphery, fields varied more than threefold in diameter, and the smallest

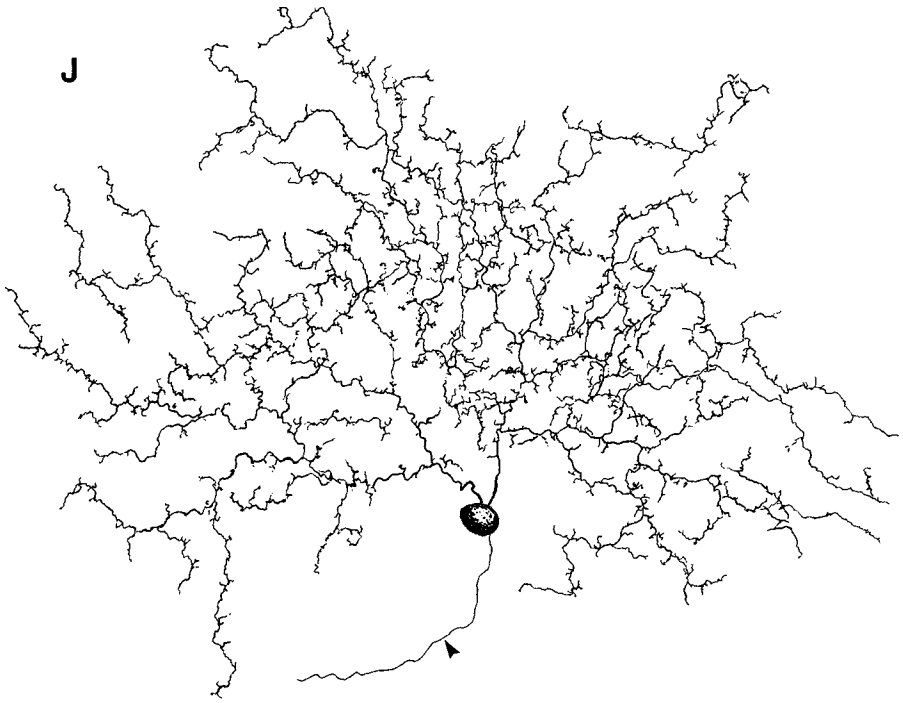

Figure 1 (Continued)

were only a bit bigger than those in the central retina. This variation was largely related to the cells' proximity to the visual streak. Cells lying nearest the streak (filled diamonds) had the smallest dendritic fields at every eccentricity whereas those farthest from the streak (open circles) had the largest fields. This relationship is evident in the drawings of Figure 1. For example, two cells drawn from the peripheral nasal visual streak (Fig. 1C,E; eccentricity >6 mm) had dendritic fields as small as one from the pericentral, nonstreak retina (Fig. 1D; eccentricity <2 mm). Likewise, three cells roughly matched in radial eccentricity (9–11 mm) varied in field size in proportion to their distance from the visual streak axis (Fig. 1C < 1G < 1H).

Quantitative analysis of this relationship indicates that outside the central 1 mm, proximity to the streak is the primary determinant of field size (Fig. 4B). Distance from the streak accounted for more of the variance in field size ($r^2 = 0.71$) than did eccentricity ($r^2 = 0.24$). Note that because the visual streak passes through the area centralis, a cell's eccentricity and its distance from the visual streak are not independent parameters. Cells near the area centralis are also, by definition, near the streak whereas peripheral cells vary widely in their distance from the streak. The pronounced influence on field size of distance from the visual streak (Fig. 4B) thus ensures at least a weak relationship between field size and eccentricity (Fig. 4A). The question thus arises of whether the small field size of zeta cells in central retina simply reflects their proximity to the streak or rather an independent influence of eccentricity. One way to disentangle these parameters is to consider the effect of eccentricity on a subset of cells all lying about the same distance from the streak axis. Consider, for example, cells lying within 0.5 mm of the streak (filled diamonds in Fig. 4A). These had nearly the same field sizes in the far nasal periphery as in the pericentral retina. However, in the central 1–2 mm, field sizes did decrease substantially. These findings suggest that eccentricity exerts a significant independent influence on field size only in the area centralis.

In the temporal hemiretina, proximity to the visual streak was also correlated with field size (Fig. 4B). The association appeared weaker, however, and that of eccentricity somewhat stronger (Fig. 4A), than it was nasally. This stronger influence of eccentricity is indicated by the relatively small dispersion of field sizes in the temporal periphery and the systematic increase in size with eccentricity for fields near the streak axis (filled diamonds, Fig. 4A, left side). Cells within 1mm of the visual streak axis were substantially larger in the temporal periphery than in the nasal periphery (eccentricities >5 mm); temporally, field diameters ranged from 235 to 557 (mean: 338 ± 133 μm s.d.), whereas nasally they ranged from 140 to 295 μm in diameter (mean: 213 ± 34 μm s.d.). Otherwise, there were no obvious nasotemporal differences in field size. Similarly, there were no apparent differences in field size between the superior and inferior hemiretinas (not shown).

Proximity to the streak appears to be a stronger determinant of field size for zeta cells than for other types of cat ganglion cells. Beta cells, for example, although clearly influenced by streak proximity, show greater variation in field size at a given distance from the streak than do zeta cells, and this variation is eccentricity dependent (Fig. 5B). Likewise, beta cells exhibit a greater correlation of field size with eccentricity than do zeta cells (Fig. 5A). In contrast to zeta cells, even beta cells within 0.5 mm of the visual streak (filled diamonds in Fig. 5A) exhibit systematic increases in field size with eccentricity, from the central retina to the far periphery.

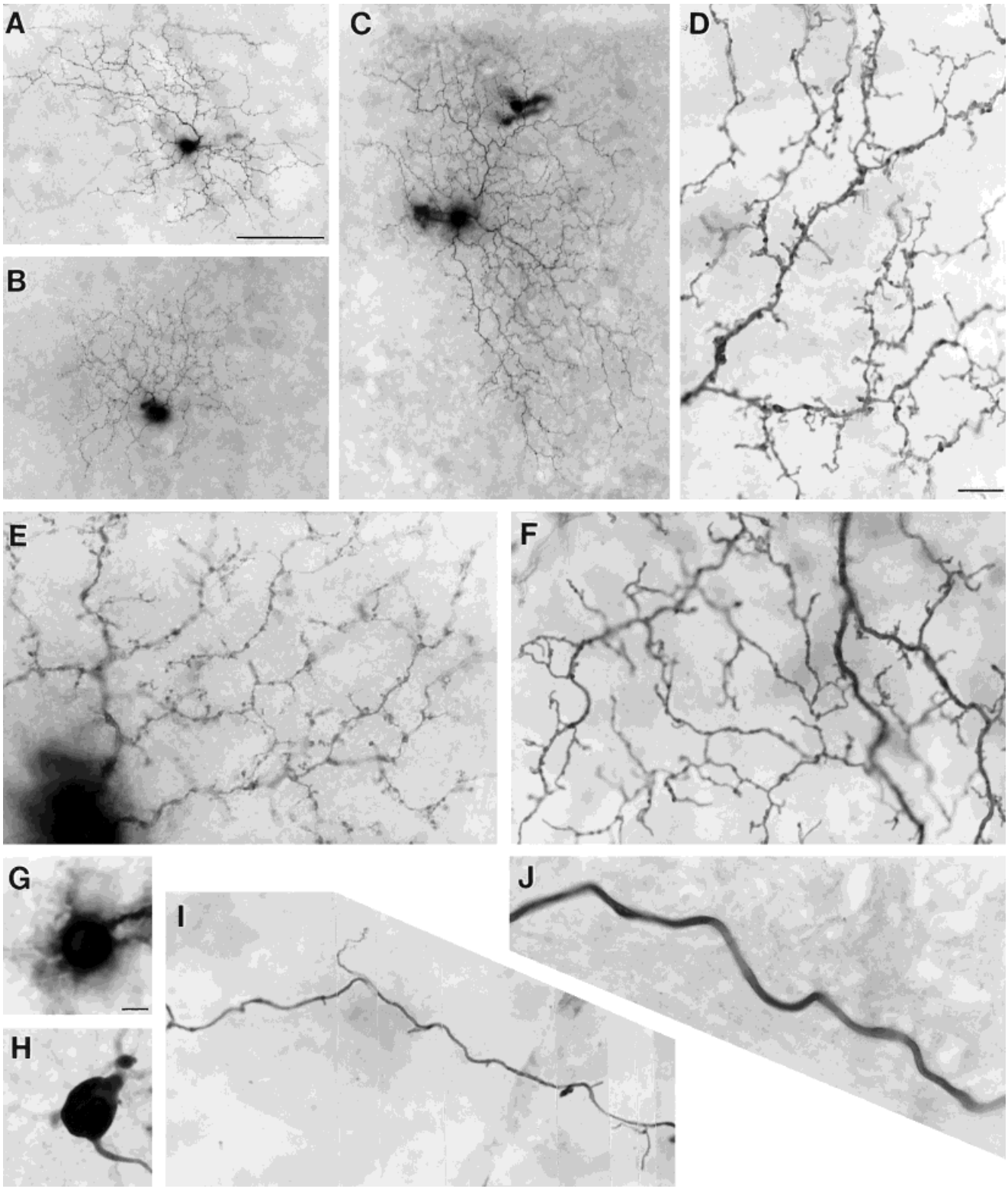

Fig. 2. A-J: Photomicrographs illustrating morphologic details of intracellularly stained zeta cells. **A–C:** Low-power photomicrographs of three typical zeta cells. **D–F:** High-power photomicrographs of dendritic arbors. **G,H:** Comparison of soma size of representative zeta (G) and beta (H) cells. **I,J:** Comparison of caliber and form of representative zeta (I) and beta (J) cell axons. Note the short collaterals emerging from the zeta cell axon. Segment shown lies 200–300 µm from the soma. Retinotopic locations were as follows, with positive distances from the area centralis (a.c.) indicating locations in the nasal hemiretina, and positive distances from the visual streak axis (v.s.a.) indicating locations in the superior hemiretina . Cell shown in A and D: +6.4 mm from a.c., +1.3 mm from v.s.a. Cell shown in B and E: -2.5 mm from a.c., +1.5 mm from v.s.a. Cell shown in C and G: -6.9 mm from a.c.; -2.9 mm from v.s.a. Cell shown in F and I: +10.9 mm from a.c., +1.5 mm from v.s.a. Cell shown in H: -5.7 mm from a.c. and +5.6 mm from v.s.a. Cell in J: +8.3 from a.c., +2.7 from v.s.a. Cells shown in A,D and F,I were labeled by retrograde transport from the contralateral superior colliculus. A camera lucida drawing of cell in F and I appears in Figure 1H. Scale bars = 100 µm in A (applies to A–C), 10 µm in D (applies to D–F,I,J), 10 µm in G (applies to G,H).

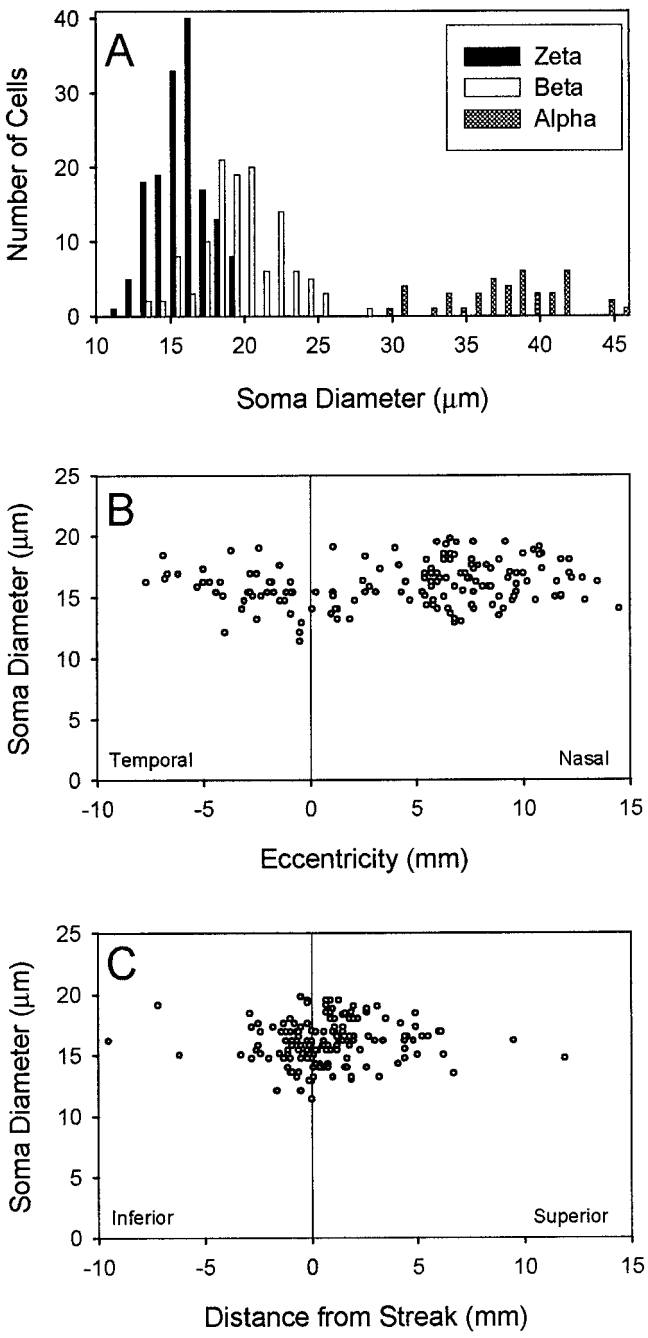

Fig. 3. Soma diameters of zeta cells plotted as a histogram (**A**) and as scatterplots as a function either of eccentricity (**B**) or of distance of the cell from the visual streak (**C**).

Figure 6 compares dendritic field sizes of zeta cells with those of the other well-established classes of cat ganglion cells. Zeta field diameters (open diamonds) are typically twice as large as those of beta cells (dots) at most retinal locations. The overlap between the zeta and beta populations in these plots is largely attributable to the reduction of two-dimensional topographic data to a unidimensional scale. Most of the apparent overlap in the nasal periphery (Fig. 6A) occurs between the relatively small zeta cells of the streak and the relatively large beta cells of the nonstreak periphery (cf. Figs. 4A and 5A). Likewise, the apparent overlap on the streak axis (Fig. 6B) occurs between zeta cells in the area centralis and beta cells in the peripheral streak (cf. Figs. 4B and 5B). When both eccentricity and streak proximity are considered in planar topography, there is almost no overlap between the populations. The one exception is in the nasal visual streak outside the central retina, where zeta and beta field sizes exhibit modest overlap. Zeta-cell fields are everywhere smaller on average than those of the delta (monoamine-accumulating) cells (filled triangles), with little overlap between the populations. Zeta fields are also far smaller than those of alpha (open circles) and epsilon cells (plus signs).

Dendritic stratification

Zeta cells had narrowly unistratified dendritic arbors. Overlapping distal branches exhibited little difference in depth, never more than a few micrometers in hydrated wholemounts, although primary dendrites could lie proximal to the main layer of arborization. The main arbor ramified slightly distal to the middle of the inner plexiform layer (IPL), in or near layer S3 and very close to the *a*/*b* sublaminar border (Fig. 7).

Zeta cells appear to be an unpaired type (Class IV of Famiglietti, 1992a) rather than comprising a paramorphic pair of types ramifying separately either in sublamina *a* or in sublamina *b*. (Paramorphic pairs are morphological types that appear virtually identical when viewed en face in the plane of the retina but that differ in the level of their dendritic stratification in the IPL. Generally, paramorphic types occur as type-*a*/type-*b* or OFF-center/ON-center counterparts, branching in sublamina *a* or sublamina *b*, respectively, of the IPL [Famiglietti and Kolb, 1976; Wässle and Boycott, 1991]). Seven pairs of zeta cells with abutting or overlapping arbors are included in our sample, one example of which is illustrated in Figure 8. In each case, dendrites of the two cells exhibited virtually complete costratification. There is less than a 1% chance of observing such consistent costratification by chance among pairs drawn from a population equally divided among *a* and *b* subtypes (binomial probability = 0.5^7; $P < .008$).

To determine the level of stratification more accurately, we used through-focus methods to compare the depths of zeta cell dendrites with those of overlapping fiducial ON and OFF alpha cells, which are known to stratify narrowly on either side of the *a*/*b* sublaminar border (see Materials and Methods for references). Zeta-cell dendrites lay sandwiched between the arbors of type *a* (OFF) alpha cells in S2 and type *b* (ON) alpha cells in inner S3 (Figs. 9–11). Zeta-cell processes occasionally exhibited apparent local costratification with those of the ON or OFF alpha cells, but were never seen proximal to the ON alpha or distal to the OFF alpha tiers (Fig. 11). Single zeta-cell arbors generally filled the gap between the alpha-cell strata. Small portions of the arbor sometimes seemed closer to one alpha stratum than the other, but this was never consistent across an entire field. There was no evidence for subtypes of zeta cells differing in their depth of arborization relative to the alpha cells. These observations were based on 28 zeta cells, of which 17 overlapped both type *a* and type *b* alpha cells and 11 overlapped one of the two types. Analysis of overlapping beta cells confirmed the view that zeta cells ramify near the *a*/*b* sublaminar border.

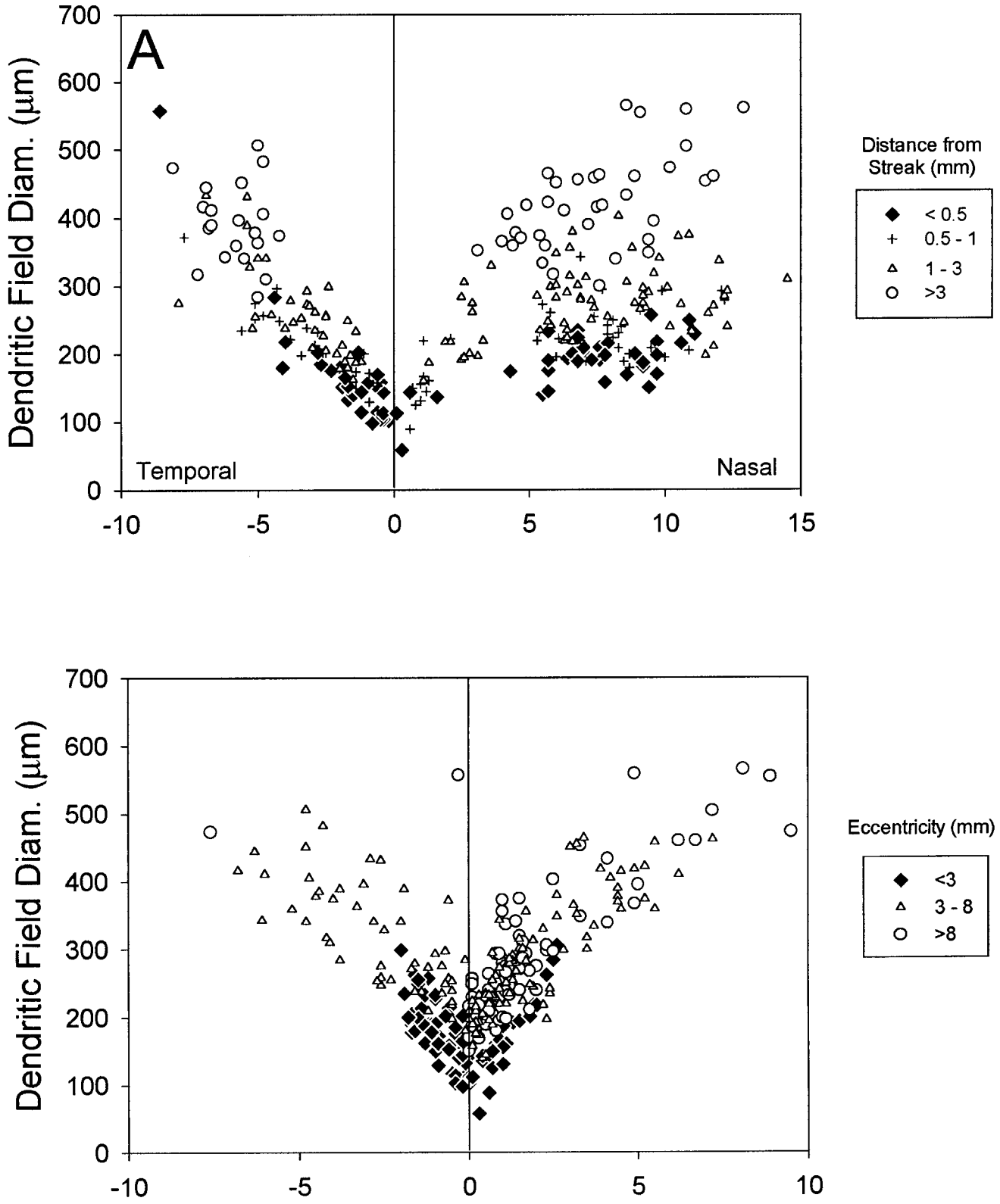

Fig. 4. Dependence of zeta-cell dendritic field size on retinal eccentricity and distance from the visual streak (in mm). **A:** Plot of field diameter as a function of eccentricity (i.e., radial distance from the area centralis). Each symbol type indicates a range of distance from the axis of the visual streak, as indicated in the key. **B:** Plot of field diameter as a function of distance from the visual streak axis. Each symbol type indicates a range of eccentricity, as indicated in the key. In both A and B, a negative sign has been assigned to distance values (abscissa) for cells in the temporal hemiretina. Note that no distinction has been made between superior and inferior retinal locations.

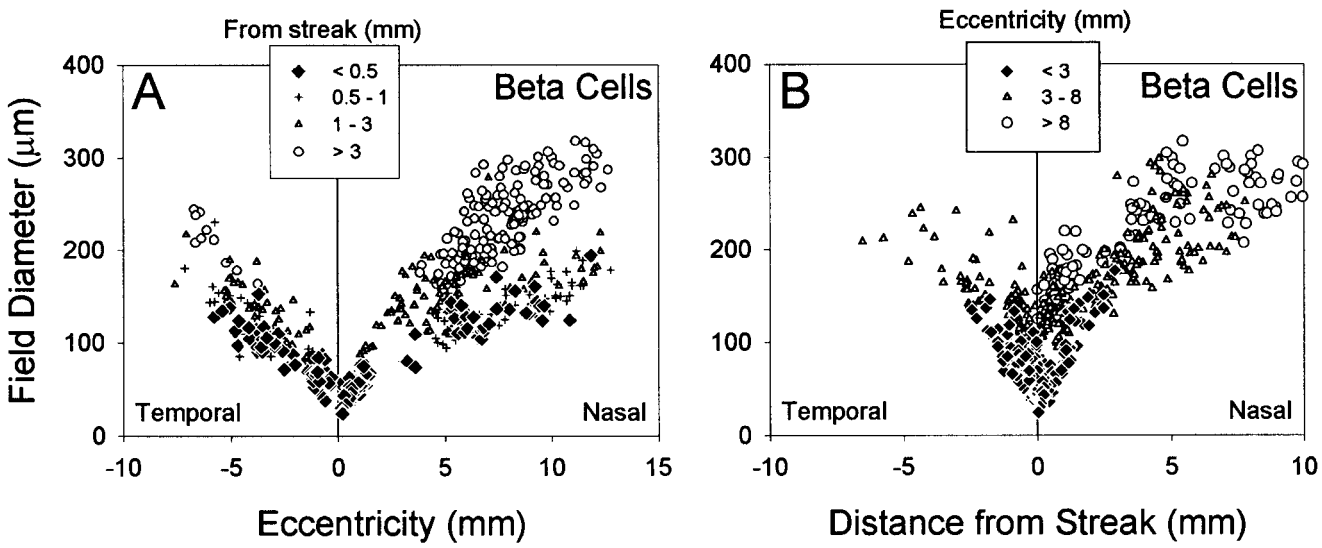

Fig. 5. **A,B:** Dependence of dendritic field size on retinal location for cat beta cells. Conventions as for Figure 4. Data drawn from Stein et al. (1996).

Zeta-cell dendrites lay almost entirely proximal to those of OFF beta cells in S1 and S2 (n = 4) and distal to those of ON betas in S3 and S4 (n = 3; Famiglietti and Kolb, 1976; Watanabe et al., 1985; McGuire et al., 1986; Weber et al., 1991), although limited costratification was sometimes apparent where these arbors abutted one another in depth.

Mosaic and density distribution

Because we lacked a method for marking zeta cells selectively, we were unable to stain all zeta cells in a patch of retina so as to characterize the spacing and overlap of their dendritic fields. However, the fact that nearby zeta cells had overlapping arbors (see above) suggests that these cells completely tile the retina. The dendritic fields in Figure 8 leave the impression of having avoided one another during development, so that their dendritic field overlap or coverage factor (dendritic field area $\times$ local density) was roughly one. However, several other zeta-cell pairs exhibited considerably more overlap (not shown). The distance between the centroids of overlapping dendritic fields may be taken as an approximation of the local spacing of dendritic fields. From this, one may derive an estimate of the spatial density of dendritic fields (or cells) by assuming cells are arranged in a hexagonal lattice. Multiplying this density estimate by the area of the dendritic field of each member of the cell pair yields two rough estimates of coverage factor. Table 1 summarizes these estimates for the seven available cell pairs. Estimated coverage ranged from 0.9 to 3.3 and averaged 1.72. The mean should probably be viewed as a lower bound estimate of true zeta-cell coverage since several of the cell pairs exhibited marginal overlap, suggesting that they may not have been nearest neighbors in the zeta-cell mosaic.

Dendritic field overlap (coverage) is topographically invariant for other ganglion cell types (Peichl and Wässle, 1979; Wässle et al., 1981; Dann et al., 1988; Dacey, 1989, 1993; Vaney, 1994; Stein et al., 1996). In other words, dendritic field areas are for each type inversely proportional to the local density of that type. By assuming such invariance for zeta cells, we generated for each of 295 cells a local estimate of zeta-cell density by dividing 1 (a rough estimate of the coverage factor; see Discussion) by the cell's dendritic field area. These density estimates, summarized in the contour plot of Figure 12A, ranged from 378 cells/mm^2 in the central retina to 4 cells/mm^2 in the nonstreak nasal periphery. Note that the absolute magnitudes of the estimated densities are very approximate, being subject to the imprecision of the estimate of coverage factor. The form of the distribution, on the other hand, is unaffected by such imprecision and presumably closely matches that of the true distribution provided that the assumption of topographic invariance of coverage is correct.

Central projections

Zeta cells were commonly encountered among cells labeled by retrograde transport from the contralateral superior colliculus (see Figs. 1C,E,G,H,I, 8 for examples). Even zeta cells in the temporal retina appeared to project to the contralateral colliculus. These were observed in a single cat in which the retrograde tracer deposit reached the rostral margin of the colliculus, which is innervated by the contralateral temporal retina (Harting and Guillery, 1976). Some of the double-labeled cells in this retina lay as far as 3.7 mm from the nasotemporal raphe. Among the many hundreds of cells that we have filled after retrograde labeling from the ipsilateral superior colliculus, there was only one clear example of a zeta cell. Furthermore, zeta cells were almost entirely lacking among dye-injected ganglion cells double labeled by retrograde transport from the lateral geniculate nucleus. We observed no clear examples among >70 cells labeled from the C-layers, >300 labeled from the A-layers, and >150 labeled from the geniculate wing. We did see two possible zeta cells among the >350 we filled after retrograde labeling from the medial interlaminar nucleus (MIN).

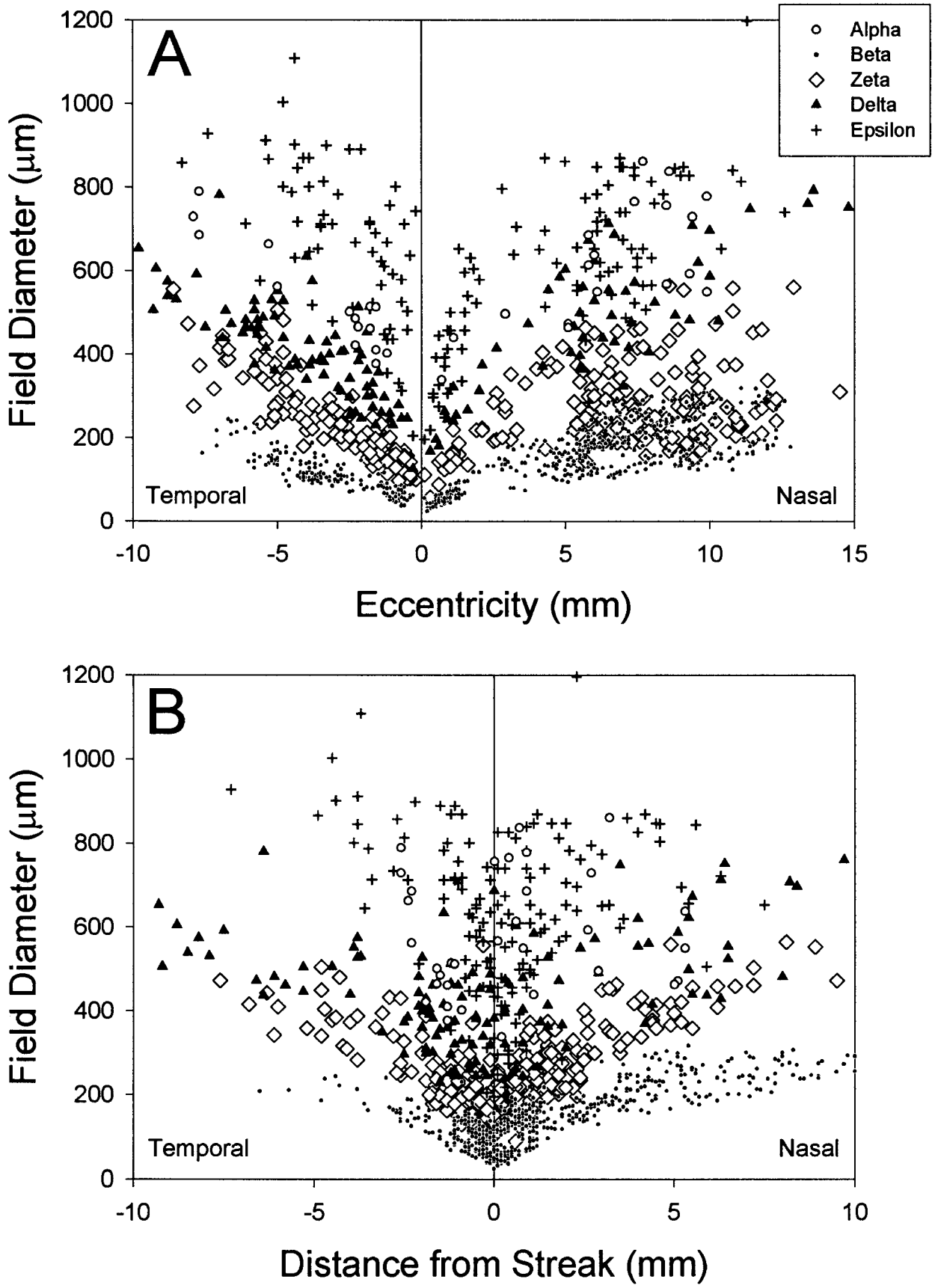

Fig. 6. **A,B:** Dependence of dendritic field size on retinal location for cat ganglion cells. Symbol types indicate morphological classes as indicated in key. Other conventions as for Figure 4.

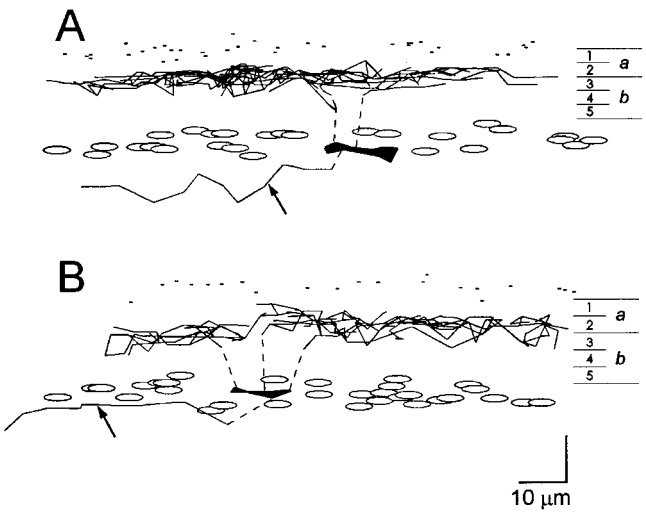

Fig. 7. Dendritic stratification of two zeta cells of the central retina as revealed by computer-generated transverse views. Dendritic branching was traced in three dimensions in hydrated wholemounts by using a computer-based microscopic reconstruction system, and then displayed as if rotated by 90° about an axis lying in the plane of the retina. These two cells were selected for reconstruction because the small size of their dendritic fields reduced the distorting effect of imperfect wholemount flatness on the uniformity of depth information in such views. Cell bodies appear as filled polygons and dendrites as straight line segments. Open ovals indicate depth of other ganglion cell bodies and dots the position of dark granules marking the outer margin of the inner plexiform layer (see Materials and Methods). Numbers at right indicate approximate depth of strata of the inner plexiform layer. Arrows indicate axons. **A:** Cell lay 0.3 mm from the area centralis and 0.3 mm from the visual streak in the superior nasal retina; a drawing of this cell appears in Figure 1A. **B:** Cell lay 0.4 mm from the area centralis on the visual streak axis in the temporal hemiretina. Scale bar = 10 μm in vertical as well as horizontal dimensions.

DISCUSSION

The present study defines a new morphological type of cat ganglion cell, the zeta cell. Its most important morphological features include a small soma, slender axon, highly branched and compact dendritic field, and stratification near the boundary of IPL sublaminae *a* and *b*. It projects contralaterally from the temporal as well as from the nasal retina and terminates primarily in the midbrain tectum rather than in the thalamus.

Relationship to other cat ganglion cell types

The morphology of the zeta cell clearly distinguishes it from four other well-studied ganglion cell types of the cat retina: the alpha, beta, delta (monoamine-accumulating), and epsilon types (Fig. 13). Two of these classes, the alpha and beta cells, consist of paramorphic pairs, with one set stratifying in sublamina *a*, and the other in sublamina *b* of the inner plexiform layer. The other two, like the zeta cell, appear to represent unpaired types (Fig. 14), but the zeta cell ramifies at the border of sublaminae *a* and *b*, whereas the epsilon cell occupies the middle of sublamina *b* and the delta cell ramifies in the distal part of sublamina *a* (Dacey, 1989; but see Wässle and Boycott, 1991). The zeta cell's soma (Fig. 3) is the smallest and its axon the finest among all of these types. Its dendritic field is, except for the beta cell, the smallest and most densely branching (Fig. 13). Zeta cells are easily distinguished from beta cells on the basis of their smaller dendritic fields (except in the peripheral nasal streak), smaller somata, finer axons and terminal dendrites, spinier, more complex dendritic fields, and distinctive patterns of dendritic stratification and axonal projection.

Besides the alpha, beta, epsilon, and delta (monoamine-accumulating) types, a rich variety of less thoroughly studied morphological forms has been depicted in earlier reports on cat ganglion cells (e.g., Boycott and Wässle, 1974; Stone and Clarke, 1980; Kolb et al., 1981; Saito, 1983; Fukuda et al., 1984; Stanford, 1987; Ramoa et al., 1988; Tootle, 1993). Among these, the only one with characteristics of the zeta type described here is the cell termed G16 by Kolb et al. (1981). This cell, of which they saw only a single example in their survey of Golgi-stained neurons, resembled the zeta cell in having a small soma and a highly branched, spiny dendritic field of the appropriate size. In addition, the arbor, like that of the zeta cell, was unistratified and ramified near the *a*/*b* sublaminar border (S3).

Likely morphological analogs of the zeta cell in other mammalian retinas

Morphological types reminiscent of the zeta cell have been described in the retinas of a variety of mammals. Among these is the ferret, which resembles the cat both phylogenetically (both are Carnivora) and in such features of retinal organization as a well-developed visual streak, a tapetum, and the presence of alpha and beta ganglion cell types. Wingate et al. (1992) described a family of ferret ganglion cells, termed tight, which they grouped on the basis of their small somata, small bushy dendritic fields, and projections to the contralateral superior colliculus but not to the thalamus or ipsilateral colliculus. Many of the cells included within this group closely resemble cat zeta cells in dendritic field size and branching pattern (especially cells i, iv, and the cell directly beneath iv in their Fig. 9; also their Fig. 10C). However, the tight group probably consists of multiple cell types, only one of which corresponds to the cat zeta cell. For example, the cells in their Figures 9iii and 10a have much more extensive dendritic overlap than do cat zeta cells. Also unlike zeta cells, tight cells exhibit wide variation in depth of dendritic stratification. Ongoing intracellular staining studies of ferret retina in our laboratory confirm the existence of a zeta-like cell in ferret retina and preliminary evidence indicates that, as in cat zeta cells, its unistratified arbor is laminated between those of overlapping ON and OFF alpha cells (Isayama et al., 1998).

Another probable counterpart of the zeta cell is a variety of "small tufted" ganglion cell in rabbit retina with a small soma, a slender axon, small dendritic field, and dendritic stratification in S3 (Famiglietti and Siegfried, 1979; Famiglietti, 1987b and unpublished observations). Like cat zeta cells, this variety of rabbit ganglion cell exhibits a pronounced reduction in dendritic field size within the visual streak, which may reflect a somewhat higher concentration of this type in the visual streak relative to other ganglion cell types (E.V. Famiglietti, unpublished observations). Within the visual streak, dendritic field diameters of these rabbit ganglion cells (E.V. Famiglietti, unpublished observations) are roughly half those of cat zeta cells when expressed in terms of linear distance, but only one-third smaller when viewed in terms of visual angle

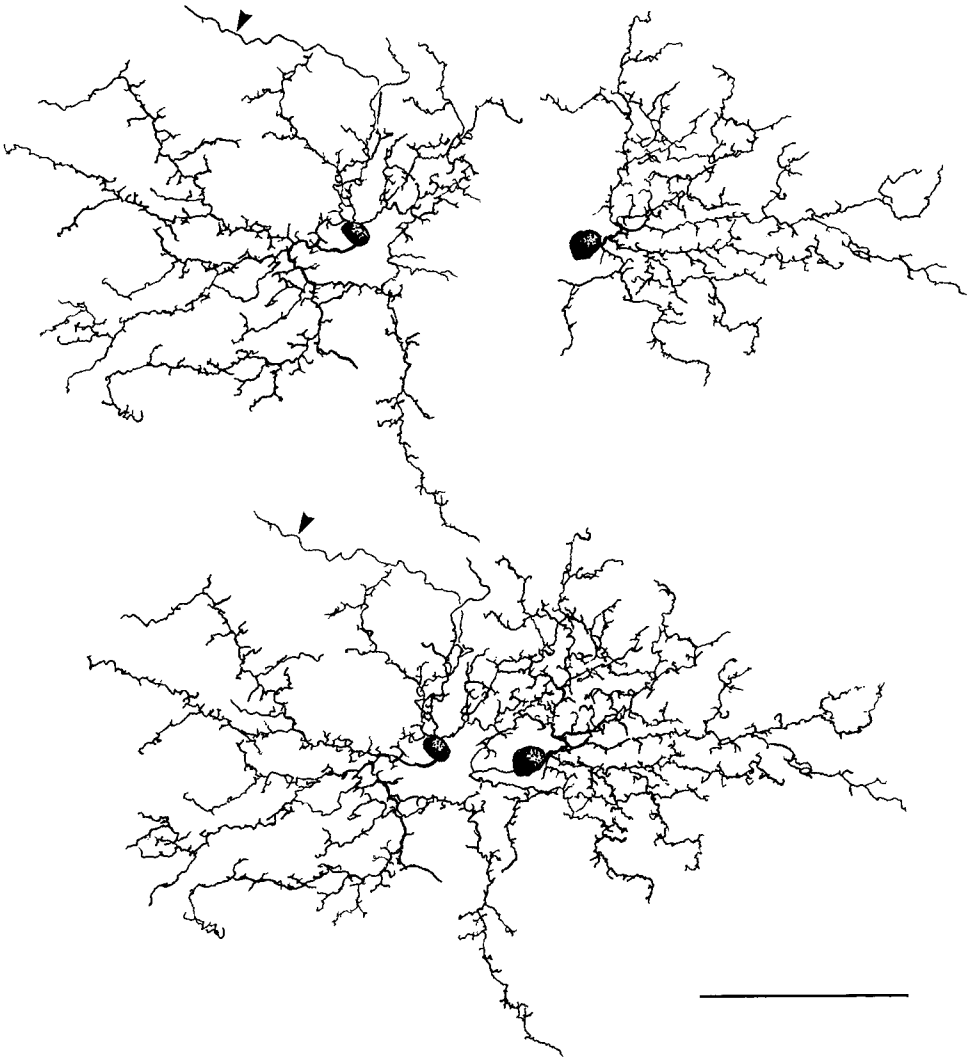

Fig. 8. Camera lucida drawings of an example of overlap between two neighboring zeta cells. The cells are shown separately above and together in their actual spatial relationship below. The cells lay 3 mm from the area centralis and 2.3 mm from the axis of the visual streak in the superior nasal retina. Both cells were labeled by retrograde transport from the contralateral superior colliculus. Arrowheads indicate axons. Scale bar = 100 μm.

subtended. A few examples of this variety of small tufted ganglion cell have been stained intracellularly after physiological identification as "local edge detectors" (Amthor et al., 1989). This physiological type has a small receptive field and a slow axonal conduction velocity (Caldwell and Daw, 1978), consistent with the small dendritic field and slender axon of the small tufted morphological type. A similar physiological type has been identified in cat retina (Cleland and Levick, 1974b; Stone and Fukuda, 1974), and it is the likely counterpart of the zeta ganglion cell (see below).

In macaque retina, Rodieck and Watanabe (1993) have described a type they term the maze cell, which exhibits some striking similarities to the cat zeta cell. It has a relatively small soma and a unistratified arbor of highly branched processes that rarely overlap. Like the zeta cell, the maze cell apparently exists as a single type, rather than as a paramorphic pair, and projects to the superior colliculus but not to the geniculate (at least, not to the parvocellular layers). The physiological properties of the maze cell are unknown, but if it proves to be analogous to the cat zeta cell and rabbit local edge detector, a prime candidate would be the ON-OFF phasic cell described in primate retina by Schiller and Malpeli (1977) and DeMonasterio (1978; particularly his type Vb).

Distribution of zeta cells

It has been suggested that ganglion cells that are neither alpha (Y) nor beta (X), sometimes termed gamma or W cells, constitute a larger fraction of all ganglion cells in the visual streak than elsewhere (Rowe and Stone, 1976). Recent evidence raises doubts that this is true for non-alpha/non-beta cells considered collectively (Hughes, 1981; Stein and Berson, 1995) or for certain distinct subtypes within that heterogeneous population (Fig. 12C; Dacey, 1989). However, the present data indicate that it may apply to at least one subtype of non-alpha, non-beta cell, namely, the zeta cell (see also Isayama et al., 1997).

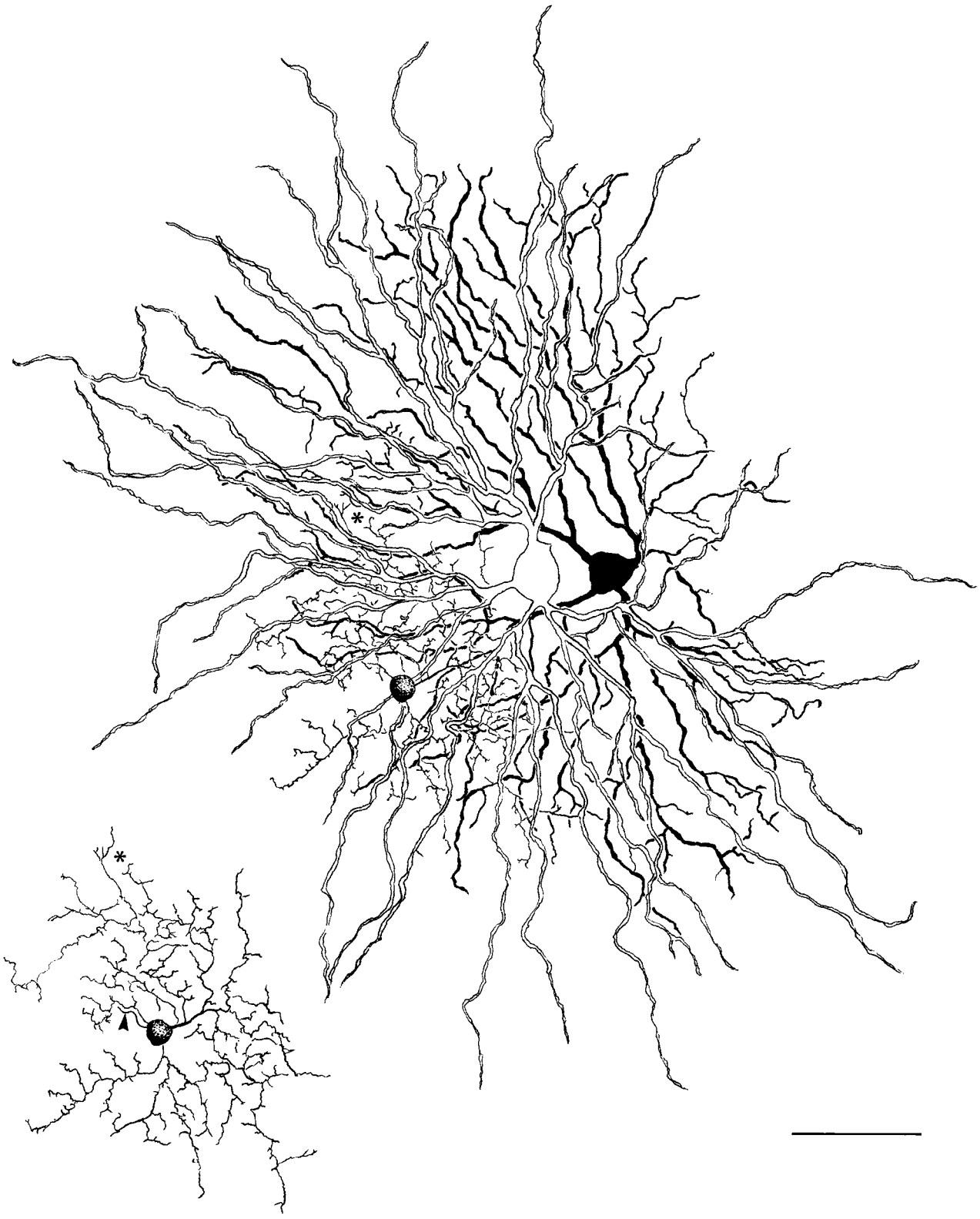

Fig. 9. Camera lucida drawings of a zeta cell and two overlapping alpha cells used for the analysis of stratification in Figs. 10 and 11A-D. One of the alpha cells (filled profile) was of the ON type ramifying in sublamina *b*, the other (hollow profile) was of the OFF variety ramifying in sublamina *a*. The zeta cell is redrawn in isolation at lower left. Asterisk indicates vicinity illustrated in photomicrographs of Figure 10. Arrowhead indicates axon. Scale bar = 100 µm.

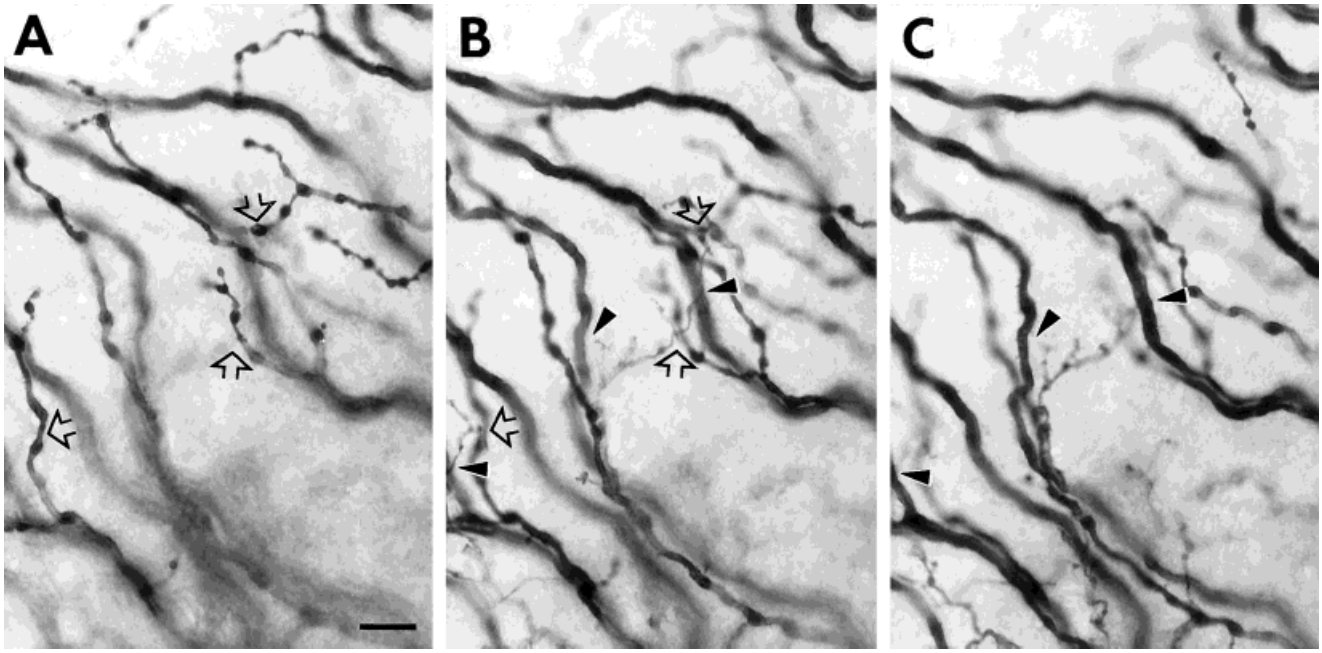

Fig. 10. **A–C:** Through-focus series of photomicrographs taken from a part of the overlapping dendritic fields shown in Figure 9 (asterisk). Plane of focus is most proximal in A and most distal in C. Open arrows in A and B indicate points of overlap or near overlap between dendrites of the ON alpha cell and those of the zeta cell. At these locations, the moderately stout, beaded ON alpha dendrites are in best focus in A, just proximal to the extremely fine zeta dendrites visible in B. Filled arrowheads in B and C indicate points of overlap or near overlap between the thick, smooth dendrites of the OFF alpha cell and the fine zeta cell dendrites. The plane of best focus for the OFF alpha dendrites (C) lies just distal to that for the zeta dendrites (B). Due to histological distortions, there is a progressive vitread displacement of the plane of best focus for all three cells as one scans from upper left to lower right in the photomicrographs. Scale bar = 10 μm.

At present, we lack a method for selectively labeling zeta cells that would permit direct assessment of their retinal distribution and total numbers. Nonetheless, inferences about the form of their density distribution can be drawn from the topography of their dendritic field sizes. To do so, we assumed, by analogy with other ganglion cell types, that the dendritic field area of zeta cells is inversely proportional to their local cell density or, in other words, that their dendritic field overlap or coverage factor (field area × local density) is a constant (Peichl and Wässle, 1979; Wässle et al., 1981; Dann et al., 1988; Dacey, 1989, 1993; Vaney, 1994; Stein et al., 1996). The coverage constant for zeta appears to be in the range of 1–2. A coverage of 1 implies complete tiling of the retina with minimal overlap, a pattern consistent with that for the cell pair shown in Figure 8 and for two other cell pairs, all of which lay near the visual streak (Table 1). Precedents for this sort of mosaic can be found in the midget ganglion cells of the human retina and the ON-OFF direction-selective ganglion cells in the rabbit (Dacey, 1993; Vaney, 1994). However, several other zeta cell pairs exhibited more dendritic field overlap. These yielded estimates of coverage closer to 2 (Table 1), more in line with data for other cat ganglion cell types (Peichl and Wässle, 1979;

Fig. 11. Quantitative analysis of depth of stratification of two zeta cells in relationship to overlapping ON and OFF alpha cell dendrites. Data in A–D are drawn from the alpha cell pair and zeta cell shown in Figures 9 and 10. **A:** Radial view of the fully reconstructed dendritic arbor of the zeta cell. Conventions as for Figure 7. Tissue distortions (see Fig. 10) in combination with the relatively large horizontal extent of the rotated field make the narrowness of stratification of the zeta cell less apparent in this reconstruction than in those of Figure 7. **B:** Absolute depth of zeta (dashes), ON-alpha (open circles), and OFF-alpha dendrites (filled circles). Data are plotted as a function of linear distance on the retina to produce a radial view comparable to that in A. Each point represents the depth of a dendrite at a point of overlap in the wholemount between a zeta-cell process and a dendrite of one (or in rare cases both) of the alpha cells. The zeta-cell dendrites (dashes) can be seen to ramify generally at a depth intermediate between those of the ON and OFF alpha, but undulations in the wholemounted retina introduce noise in the depth data that obscures the orderliness of this relationship on a local scale. **C:** Data of B replotted by normalizing each value to the depth of the overlapping zeta-cell dendrite. This flattens the tissue warp evident in A and B and reveals that the ON alpha ramifies almost entirely proximal to the zeta arbor and the OFF alpha almost entirely distal to it. **D:** Histogram replotting the normalized depth data of C. On average, the ON alpha dendrites ramified 3.5 μm ± 1.7 μm (s.d.) proximal to the zeta cell's dendrites and those of the OFF alpha 2.6 μm ± 1.5 μm (s.d.) distal to the zeta processes. E and F are drawn from a similar mutually overlapping triad of cells—a zeta cell and fiducial ON and OFF alpha cells—that lay 5.4 mm from the area centralis and 5.2 mm from the visual streak in the superior nasal retina. Only that part of the zeta field overlapped by alpha processes has been included in the analysis. **E:** Histogram of alpha cell dendritic depth, normalized as in D to the plane of zeta-cell arborization. **F:** Radial view of data in E, plotting normalized depth of alpha cell dendrites against linear distance, as in C. Again, the zeta cell's dendrites lay almost entirely between the two alpha cell tiers, on average 2.9 μm ± 0.9 μm (s.d.) distal to the dendrites of the ON alpha and 2.4 μm ± 1.0 μm (s.d.) proximal to those of the OFF alpha cell. Plus signs mark the boundary of the inner plexiform and inner nuclear layers (INL), and Xs mark the locations of cell bodies in the ganglion cell layer (GCL).

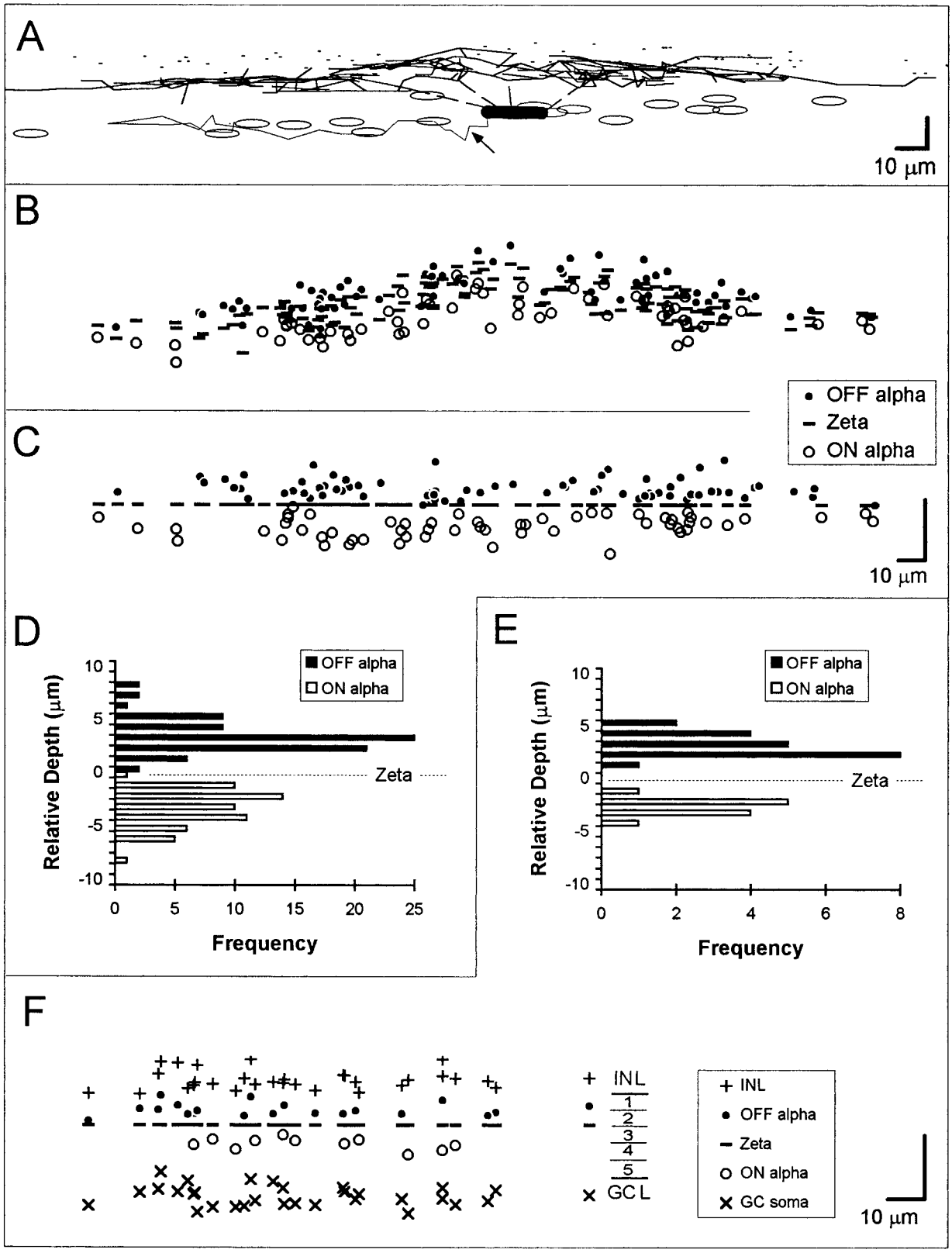
A
10 μm
B
OFF alpha
Zeta
ON alpha
C
10 μm
D
OFF alpha
ON alpha
Relative Depth (μm)
Zeta
Frequency
E
OFF alpha
ON alpha
Relative Depth (μm)
Zeta
Frequency
F
INL
1
2
3
4
5
GCL
INL
OFF alpha
Zeta
ON alpha
GC soma
10 μm

Figure 11

TABLE 1. Estimates of Anatomical Coverage for Zeta Cells

Eccentricity[1] (mm)	To streak[2] (mm)	Spacing[3] (μm)	Density[4] (cells/ mm^2)	Field diameter (μm)	Coverage
+9.6	0.0	142	57	150	1.01
				170	1.30
+7.5	+4.5	310	12	390	1.44
				415	1.63
+9.5	+1.6	204	28	319	2.22
				291	1.84
+12.1	+1.0	275	15	337	1.36
				293	1.03
+10.7	+1.3	368	9	373	0.93
				375	0.94
+3.0	+2.3	159	46	262	2.46
				197	1.39
+11.0	−1.2	124	75	238	3.33
				233	3.21
					1.72 (mean)

[1]Distance of cell pair from area centralis. Sites in nasal hemiretina are positive; those in temporal hemiretina are negative.
[2]Distance of cell pair from axis of visual streak. Sites in superior hemiretina are positive; those in inferior hemiretina are negative.
[3]Distance between centroids of the two dendritic fields in each cell pair.
[4]Spatial density of zeta cell fields estimated by assuming they form a hexagonal lattice using the formula $2/(\sqrt{3} \times S^2)$ where S is the spacing in mm of the field centroids of the two cells in the pair.

Wässle et al., 1981; Dacey, 1989; Stein et al., 1996). Further study will be needed to determine whether these discrepancies are attributable to retinal topography and field size, to the failure in some cases to inject nearest neighbors in the zeta cell mosaic, or to some other factor. The zeta cell densities shown in Figure 12A were estimated by assuming a coverage constant of 1. They thus represent lower-bound estimates of density. Substituting a higher value of coverage would have produced proportionally higher density estimates, but would not have affected the form of the distribution.

The most salient feature of the inferred distribution (Fig. 12A) is the prominent concentration of zeta cells in the visual streak. This feature is apparent to some extent in the distributions of cat ganglion cells generally (e.g., Fig. 12B and Wong and Hughes, 1987) and of individual types (e.g., beta cells: Stein et al, 1996; alpha cells: Wässle et al., 1975; Hughes, 1981; delta or monoamine-accumulating cells: Dacey, 1989). However, it appears substantially more pronounced for the zeta distribution. This is immediately apparent from a comparison of the inferred zeta- and delta-cell distributions (Fig. 12A,C). A similar distinction, although less pronounced, can be made for beta cells. In the nasal periphery (>8 mm from the area centralis), beta cells in the streak are less than four times smaller in field area than those far from the streak in the superior or inferior periphery (Stein et al., 1996). For zeta cells, such a comparison reveals nearly a ninefold difference in field area. In addition, the density gradient along the length of the streak appears shallower for zeta cells than for other types. From the middle of the area centralis to the far peripheral nasal streak, field area increases only about 16-fold for zeta cells (figured from the increase in mean diameter from 50 to 200 μm), with most of the increase occurring within a few millimeters of the area centralis. By contrast, beta cells exhibit more than twice as large an increase in field area along the streak (approximately 36-fold), with no obvious plateau in the peripheral streak (Stein et al., 1996).

The visual streak is a feature of the retinas of many different vertebrate classes. Comparative studies indicate that it is most highly developed in species whose visual habitats include a relatively flat, uncluttered terrain (Hughes, 1977). The streak is typically aligned with the retinal projection of the horizon, thus permitting high-resolution analysis of visual objects on the terrain surface. Panoramic scrutiny of visual events near the horizon is particularly useful for terrestrial animals in the detection of either prey or predators. The marked concentration of zeta cells in the visual streak points to a possible role in the analysis of such horizontally distributed terrestrial stimuli.

Relative incidence and total numbers of zeta cells

The incidence and total numbers of zeta cells can only be estimated indirectly at this point, pending the development of a selective staining method. Integration of the inferred zeta-cell density distribution (Fig. 12A) yields an estimated total of 6,500 zeta cells/retina. This amounts to 4% of the total ganglion cell population of about 160,000 (Williams et al., 1983; Chalupa et al., 1984; Wong and Hughes, 1987). We also estimated the zeta-cell fraction at a variety of retinal locations by dividing the local density of zeta cells (Fig. 12A) by the density of all ganglion cells, either as measured directly (Hughes, 1981; Stein and Berson, 1995), or as inferred from the densities and estimated fractional incidence of beta cells (Stein et al., 1996) or alpha cells (Wässle et al., 1975; Hughes, 1981). As expected, the zeta-cell fraction estimated in this way was substantially higher in the nasal visual streak (5–10%; mean 8%) than in the central (4–5%; mean 4%), temporal (3–4%; mean 3%), or nonstreak nasal retina (1–3%; mean 2%). As noted above, these values are based on lower-bound estimates of zeta-cell density. According to this analysis, zeta cells appear to be at least as common as ON-alpha, OFF-alpha, epsilon, or delta (monoamine-accumulating) ganglion cells of the cat retina (Wässle et al., 1975; Leventhal et al., 1980; Hughes, 1981; Dacey, 1989).

Physiological identity

In view of the relatively large numbers of zeta cells, it is very likely that they have been encountered in physiological studies (Cleland and Levick, 1974a,b; Stone and Fukuda, 1974; Rowe and Stone, 1976; Troy et al., 1989; Rowe and Palmer, 1995). Among the physiological types that have been described, the most likely equivalent of the zeta cell is a variety with a mixed ON and OFF receptive-field center, a transient light response, and a strong suppressive surround. It has been termed, variously, the ON-OFF center phasic W-cell (Stone and Fukuda, 1974), the local-edge detector (Cleland and Levick, 1974b), and the excited-by-contrast (Stone and Hoffmann, 1972) or impressed-by-contrast cell (Troy et al., 1989). The proposed correspondence is supported by the following observations: 1) the center mechanism of the ON-OFF phasic cell receives excitatory input from both the ON and OFF channels, and the zeta cell's dendrites stratify at the *a*/*b* sublaminar border of the IPL where they could receive input from both ON and OFF cone bipolar cells; 2) the ON-OFF phasic cell, like the zeta cell, is an unpaired type (but see Stone and Fukuda, 1974); 3) receptive field centers of ON-OFF cells are comparable in size to dendritic field sizes of zeta cells (Cleland and Levick, 1974b; Stone and Fukuda, 1974; Rowe and Palmer, 1995); 4) receptive field centers of ON-OFF cells are, despite considerable

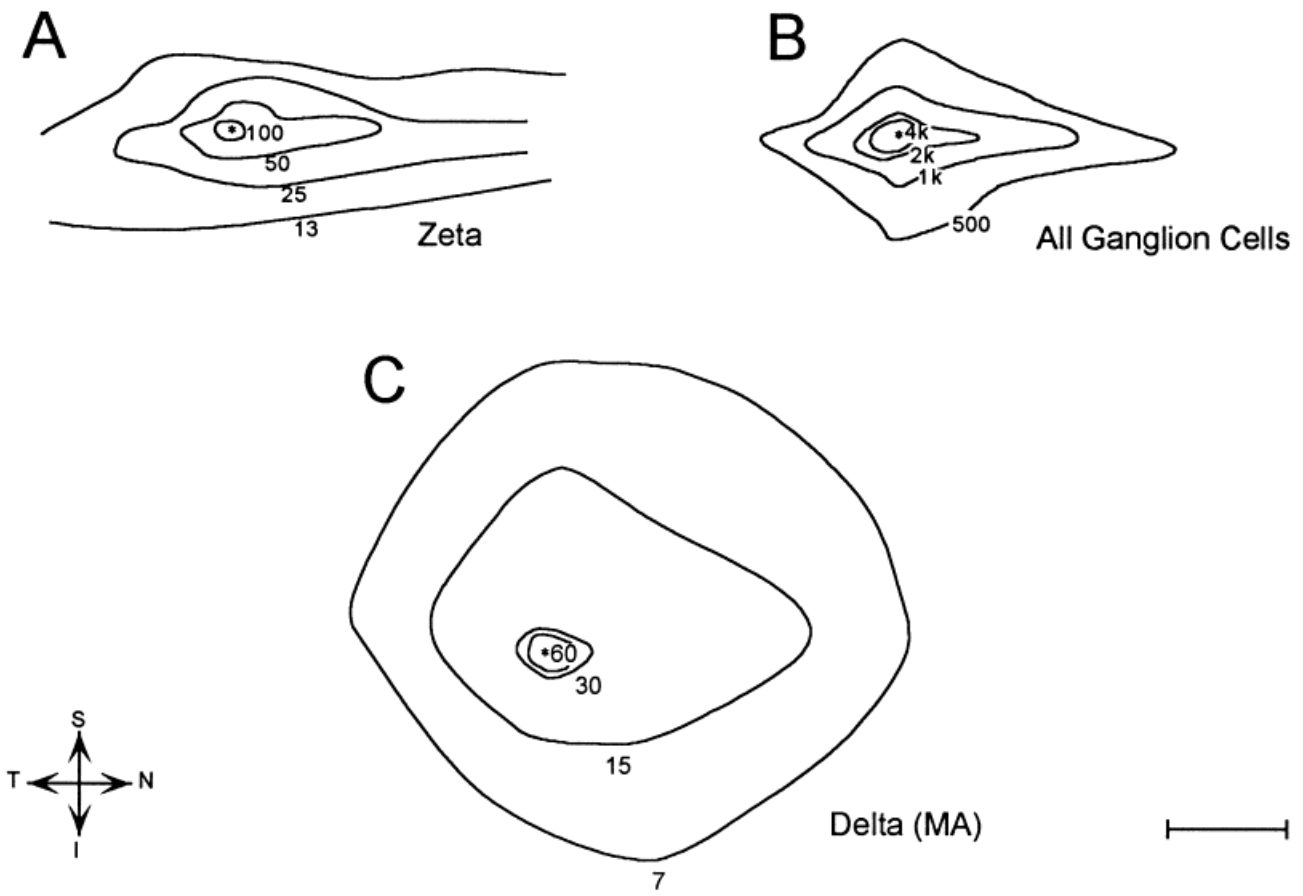

Fig. 12. Comparison of inferred retinal distribution of zeta cells (**A**) with those of all ganglion cells (**B**) and of delta (**C**; i.e., monoamine-accumulating or MA) ganglion cells of the cat retina. Data for zeta cells are inferred from zeta-cell field sizes by assuming a constant dendritic coverage (field area × local density) of 1. Asterisk indicates area centralis, where peak densities reach 378 cells/mm^2 in A; 10,000 cells/mm^2 in B; and 60 cells/mm^2 in C. S, superior; I, inferior; N, nasal; T, temporal. Data for all ganglion cells (B) redrawn from Wong and Hughes (1987; Copyright ©1987 Wiley-Liss, Inc.). Data for delta cells redrawn from Dacey (1989; Copyright ©1989 Wiley-Liss, Inc.). Reprinted by permission of Wiley-Liss, Inc., a subsidiary of John Wiley & Sons, Inc. Scale bar = 5 mm.

scatter, among the smallest for non-X, non-Y cells at any eccentricity (Cleland and Levick, 1974a,b; Stone and Fukuda, 1974), just as zeta fields are the smallest among non-alpha/non-beta types thus far identified; 5) ON-OFF cells have some of the slowest axonal conduction velocities among cat ganglion cells, just as zeta cells have among the finest axons; 6) "phasic W-cells" such as the ON-OFF type are thought to have smaller somata than other ("tonic") W-cells, just as zeta cells have smaller somata than certain non-alpha, non-beta cells such as epsilon and delta cells (Leventhal et al., 1980; Stone and Clarke, 1980; Stanford, 1987; Dacey, 1989; Pu et al., 1994); 7) ON-OFF cells almost always project contralaterally from the temporal retina (Kirk et al., 1976), just as zeta cells do; 8) many ON-OFF cells can be activated antidromically from the superior colliculus, but few from the thalamus, paralleling the zeta cell's connectivity; and 9) the cat's ON-OFF phasic W-cell is functionally very similar to the local edge detector (LED) of rabbit retina, and zeta cells resemble physiologically identified rabbit LEDs in stratification, dendritic architecture, and relative field size, soma diameter, and axon caliber (Famiglietti and Siegfried, 1979; Amthor et al., 1989; Famiglietti, unpublished observations).

Other possible candidates for the physiological counterpart of the zeta cell are the ON-OFF direction-selective type or, alternatively, the sluggish transient types. The ON-OFF direction-selective ganglion cell of cat retina has the appropriate center type, slow conduction velocity, and crossed temporal projections. However, it already has a presumptive morphological equivalent in cat retina (Famiglietti, 1987a; Berson et al., 1997), a bistratified type similar to the ON-OFF direction-selective cell in the rabbit (Famiglietti, 1981,1992b; Amthor et al., 1984, 1989; Vaney, 1994; Yang and Masland, 1994). Sluggish transient cells (also known as ON-center and OFF-center phasic W-cells) have appropriate decussation patterns and conduction velocities. On the other hand, because these cells exist as a pair of physiological types, either ON-center or OFF-center, they are expected to correspond to a paramorphic pair of morphological types stratifying separately in sublaminae *a* and *b* rather than to an unpaired type like the zeta cell. Nevertheless, as zeta-cell arbors abut or overlap the *a*/*b* sublaminar border, it is possible that some or all zeta cells receive input solely from the ON or OFF channel.

Studies directly correlating cat ganglion cell structure and function are silent on the question of the zeta cell's

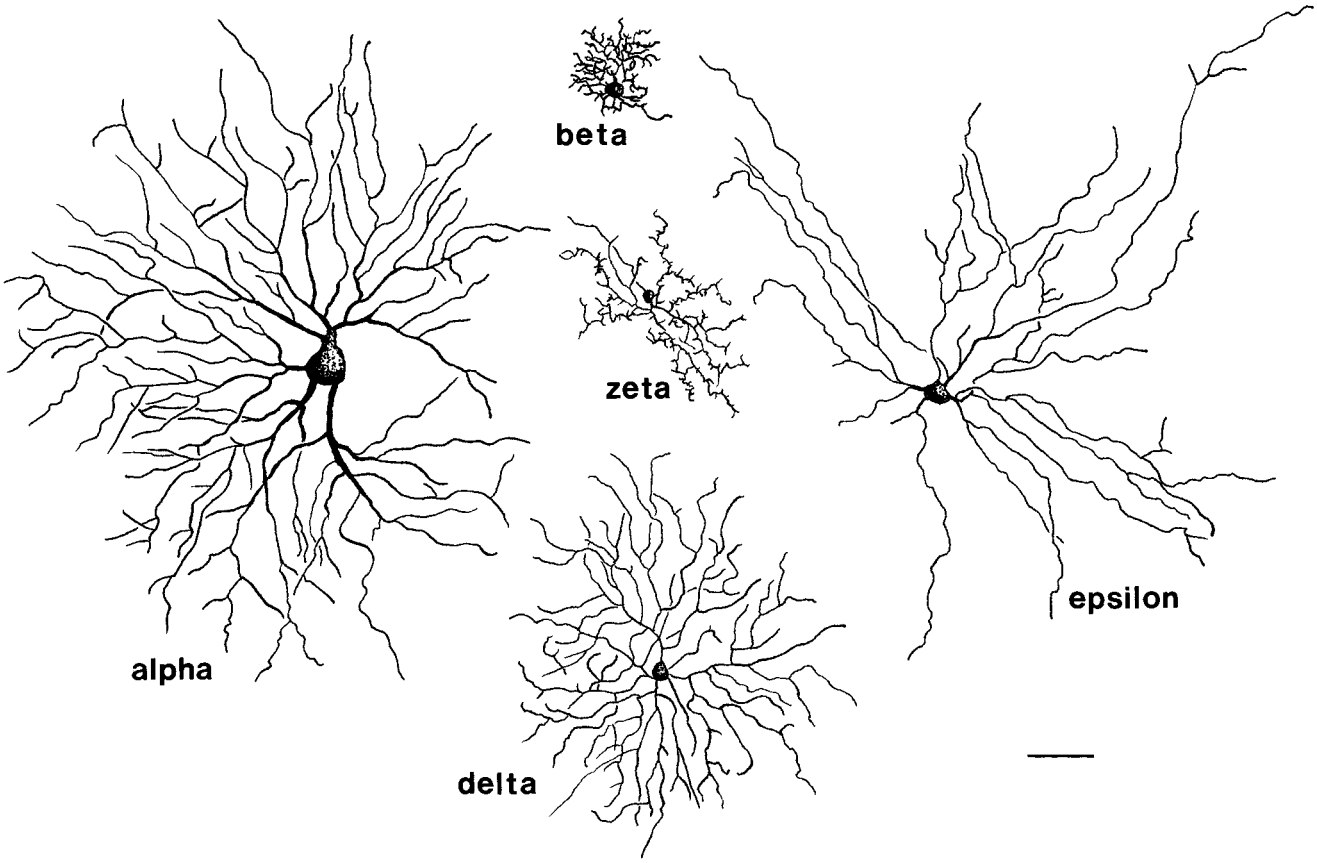

Fig. 13. Comparison of the form of the zeta cell with that of four other well-characterized morphological types of ganglion cells of the cat retina. All cells were taken from the same retinal region (approximately 6 mm eccentricity in the nasal visual streak) and stained and processed by the methods described in this study. The delta cell corresponds to the monoamine-accumulating cell (Dacey, 1989). Scale bar = 100 μm.

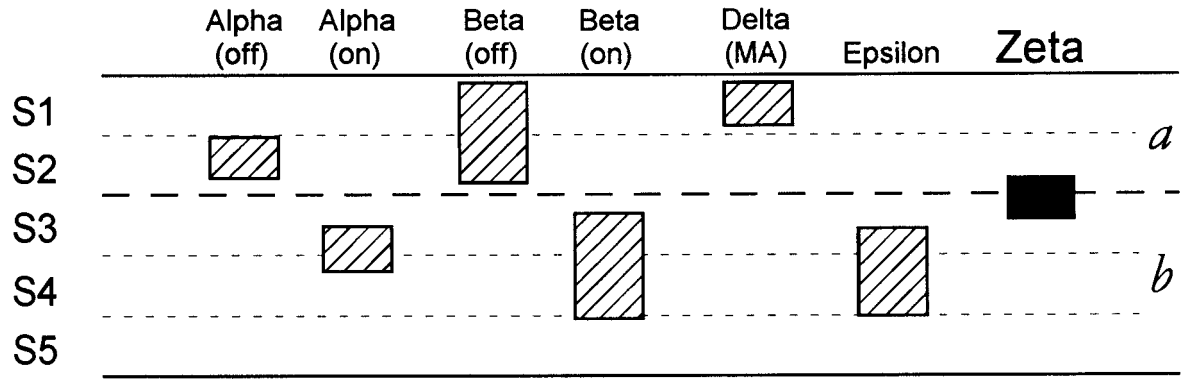

Fig. 14. Schematic summary comparing depth of dendritic stratification of zeta cells with those of the other major morphological types of ganglion cells in cat retina. Heavy dashed line marks boundary between sublamina *a* (the OFF sublayer) and sublamina *b* (the ON sublayer) of the inner plexiform layer. S1–S5 indicate sublaminae of the inner plexiform layer according to the scheme in which it is subdivided into five layers of equal thickness (Kolb et al., 1981).

functional identity (Saito, 1983; Fukuda et al., 1984; Stanford, 1987; Tootle, 1993; Pu et al., 1994). All of the recorded and injected cells are clearly distinct from the zeta cell morphologically, including two physiologically identified ON-OFF center W-cells with disparate morphology (Stanford, 1987; Tootle, 1993). The apparent morphological diversity among ON-OFF non-direction-selective ganglion cells could be related to their heterogeneity in several response properties, including transience, surround suppression, number of excitatory subfields, and balance of ON and OFF channel input (Cleland and Levick, 1974b; Stone and Fukuda, 1974; Rowe and Palmer, 1995).

Outputs

Zeta cells appear to make a substantial contribution to the retinocollicular pathway. This was to have been expected because virtually all non-beta ganglion cells in the cat project to the colliculus (Stein and Berson, 1995). Different ganglion cell classes project to different collicular layers. The zeta cell's decussation pattern and slender axon imply that it contributes to the particularly dense crossed retinal input to the uppermost part of the superficial gray layer, an input that drives collicular cells throughout the superficial gray (Berson, 1987, 1988).

Our data suggest that zeta cells make little if any contribution to the retinogeniculate projection. This distinguishes them from other non-alpha, non-beta ganglion cells (Leventhal et al., 1980; Pu and Berson, 1991; Pu et al., 1994; Isayama et al. 1997) and lends support to earlier distinctions between "thalamic-projecting" and "midbrain-projecting" ganglion cells (Rowe and Dreher, 1982; Leventhal et al., 1985). Note, however, that zeta-cell projections to the deepest C-layers or layer 3 of the MIN would have escaped detection in our studies, since for technical reasons we avoided making tracer deposits in these regions. Phasic W-cells, including some with ON-OFF centers, have been encountered in the C-laminae (Cleland et al., 1976; Wilson et al., 1976; Sur and Sherman, 1982), and these are likely to be driven by input from equivalent cell types in the retina, one or more of which may correspond to the zeta cell.

The possibility that zeta cells may have intraretinal targets is raised by the frequent appearance of fine side branches on their axons. These processes are very different from the "intraretinal terminal axons" emitted as collaterals by certain ganglion cell axons in cat and human retina, which are many millimeters long, located in the inner plexiform layer, and studded with boutons (Dacey, 1985; Peterson and Dacey, 1998; see also review of "association ganglion cells" by Rodieck, 1973). The zeta-cell axonal branches are short, terminate in or near the optic fiber, and lack obvious boutons. In these respects, they appear similar to the axonal "side branches" or intraretinal "axonal twigs" that are a common feature of many ganglion cell types in adult macaque retina (Rodieck and Watanabe, 1993) and, transiently, of immature ganglion cells in cats (Ramoa et al., 1988). It is far from clear that the zeta cell's axonal branches serve a presynaptic function. If they do, then they presumably contribute to the synaptic plexus at the junction of the ganglion cell layer and nerve fiber layer (Hughes, 1985; Koontz et al., 1989).

ACKNOWLEDGMENTS

We thank Tomoki Isayama for help with some of the intracellular filling experiments and Mike Paradiso, Cindi Rittenhouse, and James McIlwain for donations of cat eyes.

LITERATURE CITED

Amthor, F.R., C.W. Oyster, and E.S. Takahashi (1984) Morphology of ON-OFF direction-selective ganglion cells in the rabbit retina. Brain Res. *198:*187–190.

Amthor, F.R., E.S. Takahashi, and C.W. Oyster (1989) Morphologies of rabbit retinal ganglion cells with complex receptive fields. J. Comp. Neurol. *280:*97–121.

Berson, D.M. (1987) Retinal W-cell input to the upper superficial gray layer of the cat's superior colliculus: A conduction-velocity analysis. J. Neurophysiol. *58:*1035–1051.

Berson, D.M. (1988) Convergence of retinal W-cell and corticotectal input to cells of the cat superior colliculus. J. Neurophysiol. *60:*1861–1873.

Berson, D.M., T. Isayama, and M. Pu (1997) Morphology of presumed ON-OFF direction selective ganglion cell of cat retina. Soc. Neurosci. Abstr. *23:*730.

Boycott, B.B. and H. Wässle (1974) The morphological types of ganglion cells of the domestic cat's retina. J. Physiol. (Lond.) *240:*397–419.

Caldwell, J.H. and N.W. Daw (1978) New properties of rabbit retinal ganglion cells. J. Physiol. (Lond.) *276:*257–276.

Chalupa, L.M., R.W. Williams, and Z. Henderson (1984) Binocular interaction in the fetal cat regulates the size of the ganglion cell population. Neurosci. *12:*1139–1146.

Cleland, B.G. and W.R. Levick (1974a) Brisk and sluggish concentrically organized ganglion cells in the cat's retina. J. Physiol. (Lond.) *240:*421–456.

Cleland, B.G. and W.R. Levick (1974b) Properties of rarely encountered types of ganglion cells in the cat's retina and an overall classification. J. Physiol. (Lond.) *240:*457–492.

Cleland, B.G., W.R. Levick, R. Morstyn, and H.G. Wagner (1976) Lateral geniculate relay of slowly conducting retinal afferents to cat visual cortex. J. Physiol. (Lond.) *255:*299–320.

Dacey, D.M. (1985) Wide-spreading terminal axons in the inner plexiform layer of the cat's retina: Evidence for intrinsic axon collaterals of ganglion cells. J. Comp. Neurol. *242:*247–262.

Dacey, D.M. (1989) Monoamine-accumulating ganglion cell type of the cat's retina. J. Comp. Neurol. *288:*59–80.

Dacey, D.M. (1993) The mosaic of midget ganglion cells in the human retina. J. Neurosci. *13:*5334–5355.

Dann, J.F., E.H. Buhl, and L. Peichl (1988) Postnatal dendritic maturation of alpha and beta ganglion cells in cat retina. J. Neurosci. *8:*1485–1499.

DeMonasterio, F.M. (1978) Properties of ganglion cells with atypical receptive-field organization in the retina of macaques. J. Neurophysiol. *41:*1435–1449.

Dowling, J.E. (1987) The Retina: An Approachable Part of the Brain. Cambridge, MA: Belknap Press.

Famiglietti, E.V. (1981) Starburst amacrines: 2 mirror-symmetrical retinal networks. Invest. Ophthalmol. (Suppl.) *20:*204.

Famiglietti, E.V. (1987a) Starburst amacrine cells in cat retina are associated with bistratified, presumed directionally selective, ganglion cells. Brain Res. *413:*404–408.

Famiglietti, E.V. (1987b) Morphological classification of ganglion cells in rabbit retina. Soc. Neurosci. Abstr. *13:*380.

Famiglietti, E.V. (1992a) New metrics for analysis of dendritic branching patterns demonstrating similarities and differences in ON and ON-OFF directionally selective retinal ganglion cells. J. Comp. Neurol. *324:*295–321.

Famiglietti, E.V. (1992b) Dendritic co-stratification of ON and ON-OFF directionally selective ganglion cells with starburst amacrine cells in rabbit retina. J. Comp. Neurol. *324:*322–335.

Famiglietti, E.V. and H. Kolb (1976) Structural basis for 'ON' and 'OFF'-center responses in retinal ganglion cells. Science *194:*193–195.

Famiglietti, E.V. and E.C. Siegfried (1979) Quantitative analysis of ganglion cells in rabbit retina. Invest. Ophthalmol. (Suppl.) *18:*84.

Freed, M.A. and P. Sterling (1988) The ON-alpha ganglion cell of the cat retina and its presynaptic cell types. J. Neurosci. *8:*2303–2320.

Fukuda, Y., C.-F. Hsiao, M. Watanabe, and H. Ito (1984) Morphological correlates of physiologically identified Y-, X-, and W-cells in the cat retina. J. Neurophysiol. *52:*999–1013.

Harting, J.K. and R.W. Guillery (1976) Organization of retinocollicular pathways in the cat. J. Comp. Neurol. *166:*133–144

Hughes, A. (1977) Topography of vision in mammals of contrasting life style: Comparative optics and retinal organisation. In F. Crescitelli (ed.): Visual System in Evolution in Vertebrates. Handbook of Sensory Physiology, Vol. 7, No. 5, Berlin: Springer-Verlag, pp. 613–756

Hughes, A. (1981) Population magnitudes and distribution of the major modal classes of retinal ganglion cell as estimated from HRP filling and a systematic survey of the soma diameter spectra for classical neurones. J. Comp. Neurol. *197:*303–339.

Hughes, A. (1985) New perspectives in retinal organisation. In N.N Osborne and G.J. Chader (eds.): Progress in Retinal Research, Vol. 4. Oxford: Pergamon Press, pp. 243–313.

Isayama, T., D.M. Berson, and M. Pu (1997) The theta cell: A bistratified ganglion cell type in cat retina. Invest. Ophthalmol. Vis. Sci. *38:*S51.

Isayama, T., B. O'Brien, I. Ugalde, A. Frenz, V. Aurora, W. Tsiaras, J. Muller, and D. Berson (1998) Morphology of ferret retinal ganglion cells. Invest. Ophthalmol. Vis. Sci. *39:*S563.

Kirk, D.L., W.R. Levick, and B.G. Cleland (1976) The crossed or uncrossed destination of axons of sluggish concentric and non-concentric cat retinal ganglion cells, with an overall synthesis of the visual field representation. Vision Res. *16:*233–236.

Kolb, H. and R. Nelson (1993) OFF-alpha and OFF-beta ganglion cells in cat retina: II. Neural circuitry as revealed by electron microscopy of HRP stains. J. Comp. Neurol. *329:*85–110.

Kolb, H., R. Nelson, and A. Mariani (1981) Amacrine cells, bipolar cells and ganglion cells of the cat retina: A Golgi study. Vision Res. *21:*1081–1114.

Koontz, M.A., A. Hendrickson, and M.K. Ryan (1989) GABA-immunoreactive synaptic plexus in the nerve fiber layer of primate retina. Vis. Neurosci. *2:*19–25.

Leventhal, A.G. and J.D. Schall (1983) Structural basis of orientation selectivity of cat retinal ganglion cells. J. Comp. Neurol. *220:*465–475.

Leventhal, A.G., J. Keens, and I. Törk (1980) The afferent ganglion cells and cortical projections of the retinal recipient zone (RRZ) of the cat's 'pulvinar complex'. J. Comp. Neurol. *194:*535–554.

Leventhal, A.G., R.W. Rodieck, and B. Dreher (1985) Central projections of cat retinal ganglion cells. J. Comp. Neurol. *237:*216–226.

McGuire, B.A., J.K. Stevens, and P. Sterling (1986) Microcircuitry of beta ganglion cells in cat retina. J. Neurosci. *6:*907–918.

Peichl, L. and H. Wässle (1979) Size, scatter, and coverage of ganglion cell receptive field centers in the cat retina. J. Physiol. (Lond.) *291:*117–141.

Peterson, B.B. and D.M. Dacey (1998) Morphology of human retinal ganglion cells with intraretinal axon collaterals. Vis. Neurosci. *15:*377–387.

Pu, M. and D.M. Berson (1991) Morphology of ganglion cells innervating the medial interlaminar nucleus of the lateral geniculate body. Soc. Neurosci. Abstr. *17:*709.

Pu, M. and D.M. Berson (1992) A method for reliable and permanent intracellular staining of retinal ganglion cells. J. Neurosci. Methods *41:*45–51.

Pu, M., D.M. Berson, and T. Pan (1994) Structure and function of retinal ganglion cells innervating the cat's geniculate wing: An in vitro study. J. Neurosci. *14:*4338–4358.

Ramoa, A.S., G. Campbell, and C.J. Shatz (1988) Dendritic growth and remodeling of cat retinal ganglion cells during fetal and postnatal development. J. Neurosci. *8:*4239–4261.

Ramón-Moliner, E. (1962) An attempt at classifying nerve cells on the basis of their dendritic patterns. J. Comp. Neurol. *119:*211–227.

Rodieck, R.W. (1973) The Vertebrate Retina: Principles of Structure and Function. San Francisco: W.H. Freeman.

Rodieck, R.W. (1979) Visual pathways. Annu. Rev. Neurosci. *2:*193–255.

Rodieck, R.W. (1988) The primate retina. In H.D. Steklis (ed): Comparative Primate Biology, Vol. IV. Neurosciences. New York: Alan R. Liss, pp. 203–278.

Rodieck, R.W. and M. Watanabe (1993) Survey of the morphology of macaque retinal ganglion cells that project to the pretectum, superior colliculus, and parvicellular laminae of the lateral geniculate nucleus. J. Comp. Neurol. *338:*289–303.

Rowe, M.H. and B. Dreher (1982) Retinal W-cell projections to the medial interlaminar nucleus in the cat: Implications for ganglion cell classification. J. Comp. Neurol. *204:*117–133.

Rowe, M.H. and L.A. Palmer (1995) Spatio-temporal receptive-field structure of phasic W cells in the cat retina. Vis. Neurosci. *12:*117–139.

Rowe, M.H. and J. Stone (1976) Properties of ganglion cells in the visual streak of the cat's retina. J. Comp. Neurol. *169:*99–126.

Saito, A.H. (1983) Morphology of physiologically identified X-, Y-, and W-type retinal ganglion cells of the cat. J. Comp. Neurol. *221:*279–288.

Schiller, P.H. and J.G. Malpeli (1977) Properties and tectal projections of monkey retinal ganglion cells. J. Neurophysiol. *40:*428–445.

Stanford, L.R. (1987) W-cells in the cat retina: Correlated morphological and physiological evidence for two distinct classes. J. Neurophysiol. *57:*218–244.

Stein, J.J. and D.M. Berson (1995) On the distribution of gamma cells in the cat retina. Vis. Neurosci. *12:*687–700.

Stein, J.J., S.A. Johnson, and D.M. Berson (1996) Distribution and coverage of beta cells in the cat retina. J. Comp. Neurol. *372:*597–617.

Stone, J. (1983) Parallel Processing in the Visual System: The Classification of Retinal Ganglion Cells and Its Impact on the Neurobiology of Vision. New York: Plenum.

Stone, J. and Clarke, R.M. (1980) Correlation between soma size and dendritic morphology in cat retinal ganglion cells: Evidence of further variation in the gamma-cell class. J. Comp. Neurol. *192:*211–218.

Stone, J. and Y. Fukuda (1974) Properties of cat retinal ganglion cells: A comparison of W-cells with X- and Y-cells. J. Neurophysiol. *37:*722–748

Stone, J. and K.-P. Hoffmann (1972) Very slowly conducting ganglion cells in the cat's retina: A major new functional type? Brain Res. *43:*610–616.

Sur, M. and S.M. Sherman (1982) Linear and non-linear W-cells in C-laminae of the cat's lateral geniculate nucleus. J. Neurophysiol. *47:*869–884.

Tootle, J.S. (1993) Early postnatal development of visual function in ganglion cells of the cat retina. J. Neurophysiol. *69:*1645–1660.

Troy, J.B., G. Einstein, R.P. Schuurmans, J.G. Robson, and C. Enroth-Cugell (1989) Responses to sinusoidal gratings of two types of very nonlinear retinal ganglion cells of cat. Vis. Neurosci. *3:*213–223.

Vaney, D.I. (1994) Territorial organization of direction-selective ganglion cells in rabbit retina. J. Neurosci. *14:*6301–6316.

Wässle, H. and B.B. Boycott (1991) Functional architecture of the mammalian retina. Physiol. Rev. *71:*447–480.

Wässle, H., W.R. Levick, and B.G. Cleland (1975) The distribution of the alpha type of ganglion cells in the cat's retina. J. Comp. Neurol. *159:*419–438.

Wässle, H., L. Peichl, and B.B. Boycott (1981) Morphology and topography of on- and off-alpha cells in the cat retina. Proc. R. Soc. Lond.. B Biol. Sci. *212:*157–175.

Watanabe, M., Y. Fukuda, C.-F. Hsiao, and H. Ito (1985) Electron microscopic analysis of amacrine and bipolar cell inputs on Y-, X- and W-cells in the cat retina. Brain Res. *358:*229–240.

Weber, A.J., M.A. McCall, and L.R. Stanford (1991) Synaptic inputs to physiologically identified retinal X-cells in the cat. J. Comp. Neurol. *314:*350–366.

Williams, R.W. and P. Rakic (1988) Three-dimensional counting: An accurate and direct method to estimate numbers of cells in sectioned material. J. Comp. Neurol. *278:*344–352.

Williams, R.W., M.J. Bastiani, and L.R. Chalupa (1983) Loss of axons in the cat optic nerve following fetal enucleation: An electron microscopic analysis. J. Neurosci. *3:*133–144.

Wilson, P.D., M.H. Rowe, and J. Stone (1976) Properties of relay cells in the cat's lateral geniculate nucleus: A comparison of W-cells with X- and Y-cells. J. Neurophysiol. *39:*1193–1209.

Wingate, J.T., T. Fitzgibbon, and I.D. Thompson (1992) Lucifer Yellow, retrograde tracers, and fractal analysis characterise adult ferret retinal ganglion cells. J. Comp. Neurol. *323:*449–474.

Wong, R.O.L. and A. Hughes (1987) The morphology, number, and distribution of a large population of confirmed displaced amacrine cells in the adult cat retina. J. Comp. Neurol. *255:*159–177.

Yang, G. and R.H. Masland (1994) Receptive fields and dendritic structure of directionally selective retinal ganglion cells. J. Neurosci. *14:*5267–5280.